

# Wavelets and Filter Banks: Theory and Design

Martin Vetterli, *Senior Member, IEEE*, and Cormac Herley

**Abstract**—Wavelets, filter banks, and multiresolution signal analysis, which have been used independently in the fields of applied mathematics, signal processing, and computer vision, respectively, have recently converged to form a single theory. In this paper, we first compare the wavelet transform with the more classical short-time Fourier transform approach to signal analysis. Then we explore the relations between wavelets, filter banks, and multiresolution signal processing. We briefly review perfect reconstruction filter banks, which can be used both for computing the discrete wavelet transform, and for deriving continuous wavelet bases, provided that the filters meet a constraint known as regularity. Given a low-pass filter, we derive necessary and sufficient conditions for the existence of a complementary high-pass filter that will permit perfect reconstruction. Posing the perfect reconstruction condition as a Bezout identity, we then show how it is possible to find all higher degree complementary filters based on an analogy with the theory of diophantine equations. An alternative approach based on the theory of continued fractions is also given. We use these results to design highly regular filter banks, which generate biorthogonal continuous wavelet bases with symmetries.

## I. INTRODUCTION

All this time the guard was looking at her, first through a telescope, then through a microscope, and then through an opera glass.

Lewis Carroll, *Through the Looking Glass*

THE analysis of nonstationary signals often involves a compromise between how well transitions or discontinuities can be located, and how finely long-term behavior can be identified. A typical example is the choice of window length in the short-time Fourier transform. In wavelet analysis one looks at the signal at different “scales” or “resolutions”: a rough approximation of the signal might look stationary, while at a detailed level (when using a small window) discontinuities become apparent. This multiresolution, or multiscale view of signal analysis is the essence of the wavelet transform, which has recently become quite popular [1]. The goal is “to see the wood and the trees.”

The wavelet analysis is performed using a single prototype function called a wavelet, which can be thought of

as a bandpass filter. Fine temporal analysis is done with contracted (high-frequency) versions of the wavelet, while fine frequency analysis uses dilated (low-frequency) versions. The bandpass filters have thus constant relative bandwidth or “constant- $Q$ .” The importance of constant relative bandwidth when perceptual processes like the auditory system are involved has long been recognized; for example, the musical scale introduced by Bach is exponentially spaced, and subband coding of speech typically uses an octave-band splitting of signals. The multiresolution view of signals has been used in computer vision for tasks like segmentation and object recognition.

From the above discussion, it is clear that several fields have developed similar ideas independently, and it is only recently that the connections have been fully recognized. The activity in wavelets was initiated by Morlet’s work in geophysical signal processing [2]. A strong mathematical framework was built around the basic wavelet idea by the “French school” [3], [4] and is documented in the recent book by Meyer [5], which also shows the connections to earlier results in operator theory. Tutorials on wavelets are available in [6], [1], [7].

Multiresolution approaches have been popular for computer vision problems from range detection to motion estimation [8]. An important application to image coding called a pyramid [9] is closely related both to subband coding and to wavelets. Mallat used this concept of multiresolution analysis to define wavelets [10], [11], [6], and Daubechies constructed compactly supported orthonormal wavelets based on iterations of discrete filters [12]. The relation of these filters to classical maximally flat designs [13] was recently noted by Shensa [14]. In the signal processing literature, work on filter banks goes back to subband coding of speech [15], [16]. Orthogonal filter banks were first derived by Smith and Barnwell [17] and Mintzer [18], and were systematically studied by Vaidyanathan [19], [20]. The biorthogonal case, especially the linear phase case, was also studied [21]–[23].

In what follows we start by presenting a synthetic view of these diverse techniques, both as an introduction to the various tools, and as a motivation for further developments. Section II introduces the wavelet transform and compares it with the short-time Fourier transform in the continuous time case. The discrete time case and its connection to the continuous case is then explored. Section III gives a brief overview of filter bank results in the orthogonal and biorthogonal cases; and constructs biorthogonal wavelets as the limit of iterated regular filter banks (regularity means that the iterated filter converges to a

Manuscript received August 24, 1990; revised June 25, 1991. The work of M. Vetterli was supported in part by the National Science Foundation under Grants ECD-88-11111, MIP-88-08277, and MIP-90-14189. The work of C. Herley was supported in part by the National Science Foundation under Grant ECD-88-11111.

The authors are with the Department of Electrical Engineering and Center for Telecommunications Research, Columbia University, New York, NY 10027-6699.

IEEE Log Number 9201587.

continuous function). In Section IV, results on the algebraic structure of the FIR perfect reconstruction problem are presented, and these will be used to construct new wavelets. Section V presents design results of compactly supported biorthogonal symmetric wavelets based on iterated filter banks.

A certain amount of review material has been included. First, since much of the wavelet material may be unfamiliar to readers of this TRANSACTIONS we felt the review might be of interest in its own right; second, this wavelet background greatly assists the presentation of the original material that follows. The material of Sections II-D, III (from III-C onward), and IV and V is novel. Some of the main results of this paper were presented in condensed form in [24], [25].

The focus on wavelets with symmetries is motivated both by the fact that the problem was open, and for the reason that in applications like image processing linear phase is often desired [26]. Previous linear phase designs were not concerned with regularity [23], [22]; the emphasis was on equal length filters with a lattice factorization. This work specifically addresses the regularity question, and proposes new techniques to produce regular designs. The importance of regularity for signal processing applications is still an open question. While it is an elegant mathematical result on the relation between continuous and discrete systems, most filters used in signal processing applications are "almost regular," when a finite number of iterations is involved. Settling this question will of course require substantial experimental evidence, and is beyond the scope of this paper.

To give an idea of the effect of phase, we show in Fig. 1 the continuous wavelet transform plots of a burst of a sine wave analyzed with a) a symmetric wavelet designed in Section V-A, and b) an asymmetric wavelet designed in [12]. The horizontal axis represents time, while the vertical represents the log of scale (scale being the inverse of frequency). Scale increases from top to bottom; and the range is eight octaves for each of the plots. In other words, the scale of the analyzing wavelet is smallest at the top of the plot; and the largest scale is  $2^8$  times the smallest. Note that unlike the Morlet wavelet used in [27], both of these wavelets are real, so magnitude and phase information do not have to be separately computed. For signal analysis, unlike coding, it is not necessary to use perfect reconstruction systems, since the representation is generally highly oversampled, and thus the continuous wavelet transform example shown is for illustration purposes only.

During the completion of this work, we became aware of results developed independently by other researchers. Cohen *et al.*'s work on biorthogonal bases of wavelets [28], while of a more mathematical nature, leads to very similar designs. A recent manuscript by Rioul [29], while mainly focused on the orthogonal case, contains also some results on biorthogonal systems, as well as the connection with filter banks.

*Notation:* The set of real numbers will be represented

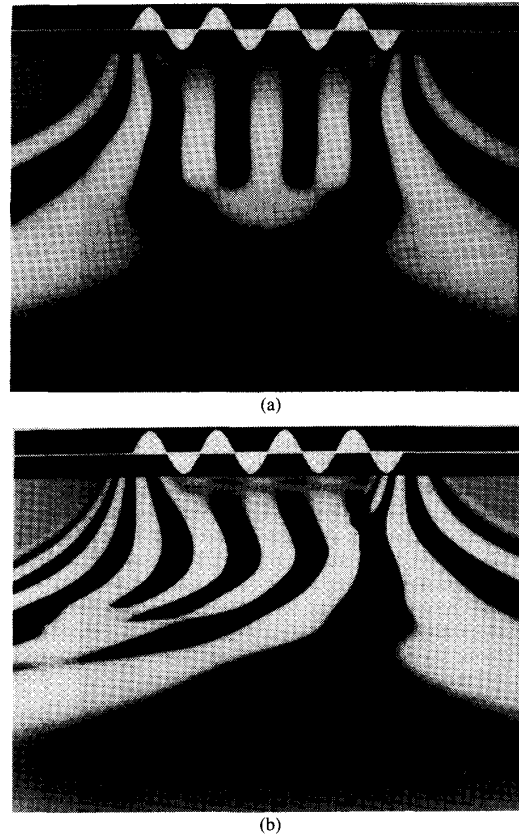


Fig. 1. Continuous wavelet transform plots. The signal is shown on top; the axes are time horizontally, and log scale vertically. (a) Sineburst analyzed using symmetric wavelet. (b) Sineburst analyzed using asymmetric wavelet.

by  $R$  ( $R^+$  being the set of positive reals), the set of integers is  $Z$ . The inner product over the space of square-summable sequences  $l^2(Z)$  is

$$\langle a(n), b(n) \rangle = \sum_{n=-\infty}^{\infty} a^*(n)b(n)$$

where  $a(n), b(n) \in l^2(Z)$ , and the asterisk \* denotes complex conjugation. We define  $\|a(n)\|_2^2 = \langle a(n), a(n) \rangle$ , and  $\|a(n)\|_\infty = \max_n a(n)$ . Similarly, over the space of square-integrable functions  $L^2(R)$  we have the inner product:

$$\langle f(x), g(x) \rangle = \int_{-\infty}^{\infty} f^*(x)g(x) dx$$

where  $f(x), g(x) \in L^2(R)$ . The norm is given by  $\|f(x)\|_2^2 = \langle f(x), f(x) \rangle$ . The  $z$  transform of a sequence is defined by  $H(z) = \sum_{n=-\infty}^{\infty} h(n)z^{-n}$ . The time reversed version of a sequence which is nonzero for  $n = 0, 1, \dots, L-1$  is  $\tilde{h}(n) = h(L-1-n)$ . We shall use the notation  $\{h(n)\} = [h(0), h(1), \dots, h(L-1)]$  when we want to indicate the coefficients of an FIR filter. Note that we will consider only filters with real coefficients, unless otherwise specified.

Matrix and vector quantities will be denoted by bold-

face symbols; the asterisk \* will denote Hermitian transposition, which, since we will consider only matrices with real coefficients, is equivalent to ordinary transposition.

II. WAVELETS, MULTIREOLUTION SIGNAL PROCESSING, AND FILTER BANKS

A. The Wavelet Transform

Analysis of signals using appropriate basis functions goes back at least as far as Fourier who used complex sinusoids. The Fourier transform of a continuous time signal  $x(t)$  is  $X_F(\omega) = \langle e^{j\omega t}, x(t) \rangle$ . A difficulty that has often been cited with this approach is that, because of the infinite extent of the basis functions, any time-local information (e.g., an abrupt change in the signal) is spread out over the whole frequency axis. Gabor addressed this problem by introducing windowed complex sinusoids as basis functions [30]. This leads to the doubly indexed windowed Fourier transform:

$$X_{WF}(\omega, \tau) = \int_{-\infty}^{\infty} e^{-j\omega t} w(t - \tau)x(t) dt \quad (1)$$

where  $w(\cdot)$  is an appropriate window like a Gaussian. That is,  $X_{WF}(\omega, \tau)$  is the Fourier transform of  $x(t)$  windowed with  $w(\cdot)$  shifted by  $\tau$ . Equivalently, the basis functions are modulated versions of the window function (see Fig. 2(a)) [31]. The major advantage of the windowed or short-time Fourier transform (STFT) is that if a signal has most of its energy in a given time interval  $[-T, T]$  and frequency interval  $[-\Omega, \Omega]$ , then its STFT will be localized in the region  $[-T, T] \times [-\Omega, \Omega]$ , and will be close to zero in time and frequency intervals where the signal has little energy. A limitation of the STFT is that, because a single window is used for all frequencies, the resolution of the analysis is the same at all locations in the time-frequency plane (see Fig. 2(b)).

Of course, the uncertainty principle excludes the possibility of having arbitrarily high resolution in both time and frequency, since it lower bounds the time-bandwidth product of possible basis functions by  $\Delta T \cdot \Delta\Omega \geq (1/4\pi)$ , where  $(\Delta T)^2$  and  $(\Delta\Omega)^2$  are the variances of the absolute values of the function and its Fourier transform, respectively [32]. However, by varying the window used, one can trade resolution in time for resolution in frequency. In order to isolate discontinuities in signals one would like to have some basis functions which are very short, while some long ones are required to obtain fine frequency analysis. An intuitively appealing way to achieve this is to have short high frequency basis functions, and long low frequency ones. This is exactly what is achieved with the wavelet transform, where the basis functions are obtained from a single prototype wavelet by translation and dilation/contraction [12], [11], [3], [4]:

$$h_{a,b}(t) = \frac{1}{\sqrt{a}} h\left(\frac{t-b}{a}\right) \quad (2)$$

where  $a \in R^+$ ,  $b \in R$ . For large  $a$ , the basis function becomes a stretched version of the prototype wavelet, that

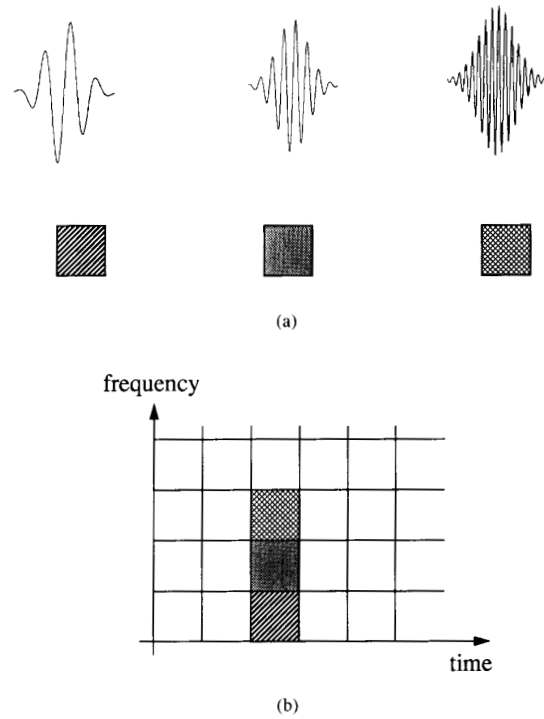


Fig. 2. Basis functions and time frequency resolution of the short-time Fourier transform (STFT). (a) Basis functions. (b) Coverage of time-frequency plane.

is a low frequency function, while for small  $a$ , the basis function becomes a contracted wavelet, that is a short high frequency function (see Fig. 3(a)).

The wavelet transform (WT) is defined as

$$X_W(a, b) = \frac{1}{\sqrt{a}} \int_{-\infty}^{\infty} h^*\left(\frac{t-b}{a}\right) x(t) dt. \quad (3)$$

The time-frequency resolution of the WT involves a different tradeoff to the one used by the STFT: at high frequencies the WT is sharper in time, while at low frequencies, the WT is sharper in frequency (see Fig. 3(b)). The middle functions depicted in Figs. 2(a) and 3(a) are identical, and hence the time-frequency resolutions of the two methods are the same at that frequency.

Obviously, both the STFT in (1) and the WT in (3) are highly redundant when the parameters  $(\omega, \tau)$  and  $(a, b)$  are continuous. Therefore the transforms are usually evaluated on a discrete grid on the time-frequency and time-scale plane, respectively, corresponding to a discrete set of continuous basis functions. The question arises as to whether there is a grid such that the set of basis functions constitutes an orthonormal basis; which of course implies that there is no redundancy. Unfortunately, for the STFT, this can happen only if  $w(\cdot)$  is badly localized in either time or frequency [33], which is the reason that the STFT is usually "oversampled" (a redundant set of points is used), so that better behaved window functions can be used. In the wavelet transform case, however, it is pos-

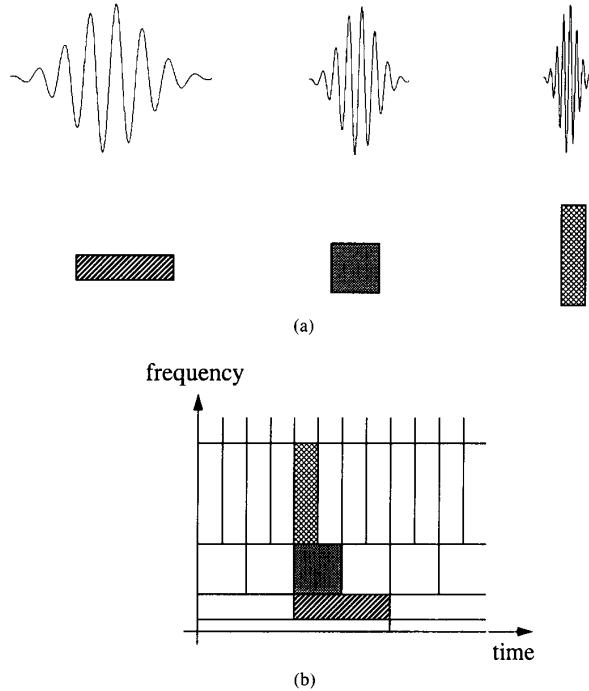


Fig. 3. Basis functions and time-frequency resolution of the wavelet transform (WT). (a) Basis functions. (b) Coverage of time-frequency plane.

sible to design "nice" functions  $h(\cdot)$  such that the set of translated and scaled versions of  $h(\cdot)$  forms an orthonormal basis. By "nice" we mean that the function should be at least continuous, perhaps with continuous derivatives also. Let us discretize the translation and dilation/contraction parameters of the wavelet in (2):

$$h_{mn}(t) = a_0^{-m/2} \cdot h(a_0^{-m}t - nb_0),$$

$$m, n \in \mathbb{Z}, \quad a_0 > 1, \quad b_0 \neq 0$$

which corresponds to  $a = a_0^m$  and  $b = na_0^m b_0$ . Note that the translation step depends on the dilation, since long wavelets are advanced by large steps, and short ones by small steps. On this discrete grid, the wavelet transform is thus

$$X_W(m, n) = a_0^{-m/2} \int_{-\infty}^{\infty} h(a_0^{-m}t - nb_0)x(t) dt. \quad (4)$$

Of particular interest is the discretization on a dyadic grid, which occurs for  $a_0 = 2$ ,  $b_0 = 1$ . It is possible to construct functions  $h(\cdot)$  so that the set

$$h_{mn}(t) = a_0^{-m/2} \cdot h(a_0^{-m}t - nb_0),$$

$$m, n \in \mathbb{Z}, \quad a_0 = 2, \quad b_0 = 1 \quad (5)$$

is orthonormal. That is,

$$\langle h_{mn}(t), h_{kl}(t) \rangle = \delta_{mk} \delta_{nl}.$$

A classic example is the Haar basis (which is not contin-

uous, but is of interest because of its simplicity), where:

$$h(t) = \begin{cases} 1 & 0 \leq t < 1/2 \\ -1 & 1/2 \leq t < 1 \\ 0 & \text{otherwise.} \end{cases}$$

The orthonormality is easily verified since at a given scale, translates are nonoverlapping, and because of the scale change by 2, the basis functions are orthogonal across scale. The Haar basis is shown in Fig. 4(a). However, the Haar function is discontinuous, and is not generally appropriate for signal processing. A continuous set of basis functions is given in Fig. 4(b). These functions are obtained from a compactly supported wavelet constructed by Daubechies [12], using a length 4 FIR filter. Longer filters lead to smoother functions. It is interesting to note that the translates and dilates of the functions in both Figs. 4(a) and (b) form orthonormal bases for  $L^2(\mathbb{R})$  functions. The purpose of the present paper is to design other continuous wavelets, having additional properties like linear phase.

### B. Multiresolution Signal Processing

From a signal processing point of view, a wavelet is a bandpass filter. In the dyadic case given in (5), it is actually an octave band filter. Therefore the wavelet transform can be interpreted as a constant- $Q$  filtering with a set of octave-band filters, followed by sampling at the respective Nyquist frequencies (corresponding to the bandwidth of the particular octave band). It is thus clear that by adding higher octave bands, one adds details, or resolution, to the signal. Mallat [10], [11] and Meyer [5] introduced the concept of multiresolution analysis and used it to construct orthonormal bases of wavelets. This multiresolution view can be interpreted as a successive approximation procedure.

We will give a simple but intuitive explanation of multiresolution and successive approximation. Call  $V_0$  the space of all band-limited functions with frequencies in the interval  $(-\pi, \pi)$ . Then the set of functions

$$\phi(x - k) = \text{sinc}(x - k) = \frac{\sin(\pi(x - k))}{\pi(x - k)} \quad k \in \mathbb{Z} \quad (6)$$

forms an orthonormal basis for  $V_0$ . Similarly, call  $V_{-1}$  the space of band-limited functions with frequencies in the interval  $(-2\pi, 2\pi)$ . Clearly, the set  $\sqrt{2} \cdot \text{sinc}(2x - k)$ ,  $k \in \mathbb{Z}$  is an orthonormal basis for  $V_{-1}$ . Also,

$$V_0 \subset V_{-1}. \quad (7)$$

In particular, if  $x(t) \in V_0$ , then  $x(2t) \in V_{-1}$ . Now, call  $W_0$  the space of bandpass functions with frequencies in the interval  $(-2\pi, -\pi) \cup (\pi, 2\pi)$ . Then

$$V_{-1} = V_0 \oplus W_0 \quad (8)$$

that is,  $W_0$  is the orthogonal complement in  $V_{-1}$  of  $V_0$ . In other words,  $V_{-1}$  is equivalent to  $V_0$  plus some added de-

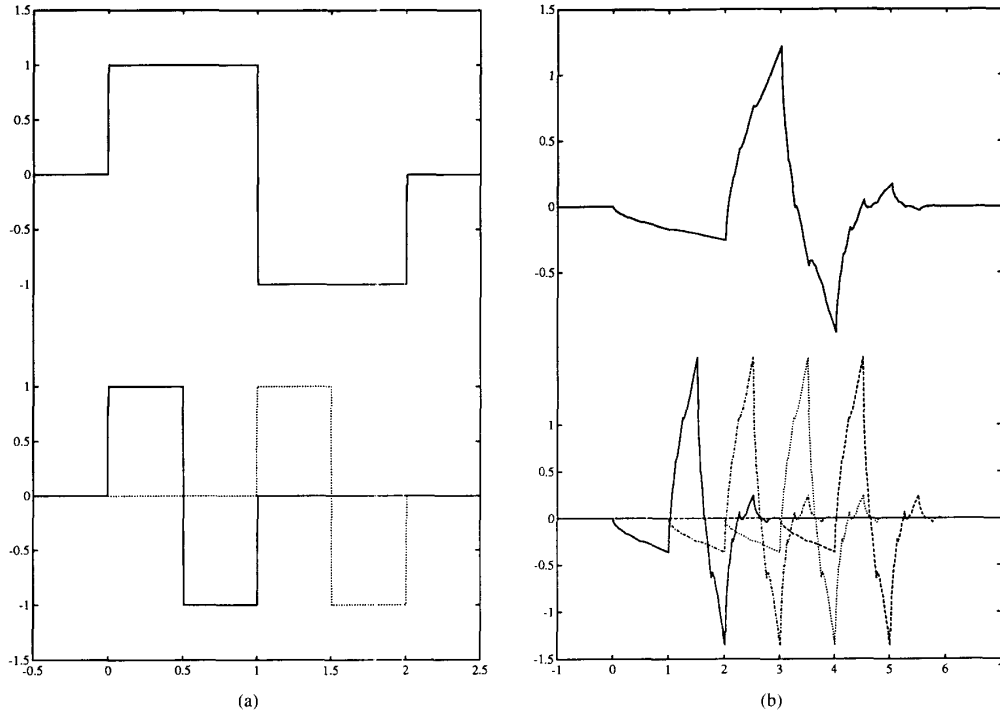


Fig. 4. Orthogonal system of scaled and translated wavelets (two scales only are shown). (a) Haar wavelet. (b) Daubechies's wavelet based on a length-4 regular filter.

tail corresponding to  $W_0$ . For completeness  $\cos(\pi x)$  has to be included in  $V_0$ , and  $\sin(\pi x)$  in  $W_0$ . From the above it is clear, by scaling, that if  $V_i$  is the space of band-limited functions with frequencies in the interval  $(-2^{-i}\pi, 2^{-i}\pi)$ , then we get relations similar to (7) and (8):

$$V_i \subset V_{i-1} \quad i \in \mathbb{Z} \tag{9}$$

$$V_{i-1} = V_i \oplus W_i \quad i \in \mathbb{Z} \tag{10}$$

where  $W_i$  is the space of bandpass functions with frequencies in the interval  $(-2^{-i+1}\pi, -2^{-i}\pi) \cup (2^{-i}\pi, 2^{-i+1}\pi)$ . Moreover, we have:

$$\dots V_2 \subset V_1 \subset V_0 \subset V_{-1} \subset V_{-2} \dots$$

and, by iterating (10)

$$V_i = W_{i+1} \oplus W_{i+2} \oplus W_{i+3} \oplus \dots \tag{11}$$

and, finally, the direct sum of all  $W_j$ 's,  $j = i + 1, \dots, \infty$ , is equivalent to the space of square integrable functions band limited to  $(-2^{-i+1}\pi, 0) \cup (0, 2^{-i+1}\pi)$ .

Let us now construct the wavelet that will span  $W_0$ . First the set  $\{\phi(x - k), k \in \mathbb{Z}\}$  given by (6) constitutes a basis for  $V_0$ . Thus  $\{\sqrt{2} \phi(2x - k), k \in \mathbb{Z}\}$  constitutes a basis for  $V_{-1}$ . Now, in the sampled version of  $V_{-1}$ ,  $\phi(x)$  is given by the perfect halfband low-pass filter with impulse response:

$$\sqrt{2} c_n = \frac{\sin(\pi n/2)}{\pi n/2} \equiv \text{discrete halfband filter.} \tag{12}$$

That is,  $\phi(x)$  can be written as

$$\phi(x) = \sum_{n=-\infty}^{\infty} c_n \phi(2x - n)$$

since it is the interpolation, by  $\phi(2x)$ , of the perfect halfband low-pass filter. Note that  $\phi(x)$  and  $c_n$  are both symmetric.  $\phi(x)$  is called a *scaling function* because it derives an approximation in  $V_0$  of signals in  $V_{-1}$ . In  $V_{-1}$ , the orthogonal complement  $W_0$  to  $V_0$  is given by the halfband high-pass signals. In the sampled domain, this is given by the halfband low-pass (12) modulated by  $(-1)^n$ , and shifted by one (to include  $\sin(\pi x)$ ). Thus,  $\psi(x)$  is the interpolation thereof, that is,

$$\psi(x) = \sum_{n=-\infty}^{\infty} (-1)^n c_{-n+1} \phi(2x - n). \tag{13}$$

Note that since the  $c_n$ 's are symmetric we can reverse the sign as above, which we do for later convenience. Now

$$\phi(x - k) \perp \psi(x - k) \tag{14}$$

since they cover disjoint regions of the spectrum. Also

$$\langle \psi(x - k), \psi(x - l) \rangle = \delta_{kl}$$

because the translates of  $\phi(2x - n)$  in (13) are even, and thus the sign change is cancelled. Then the inner product reduces to  $\langle \phi(x - k), \phi(x - l) \rangle = \delta_{kl}$ . It can be shown that the  $\psi(x)$ 's span  $W_0$ , and therefore,  $\psi(x)$  and its integer translates form an orthonormal basis for  $W_0$ . Thus, the wavelet for this bandpass example is given by  $\psi(x)$ .

Pictorially the situation is as shown in Fig. 5. Fig. 5(a) shows the imbrication of  $V_1 \subset V_0 \subset V_{-1}$ , and (b) shows the added bandpass spaces  $W_i$ . While the above example may seem artificial, and leads to a wavelet  $\psi(x)$  which is of infinite extent and has slow decay, the situation is conceptually the same for all orthonormal wavelet bases [12]. Fig. 6 shows the corresponding division of the spectrum for a wavelet that has compact support. In particular, given an orthonormal basis for  $V_0$  made up of  $\phi(x)$  and its integer translates, then, we can find coefficients  $c_n$  such that

$$\phi(x) = \sum_{n=-\infty}^{\infty} c_n \phi(2x - n) \quad (15)$$

because  $V_0 \subset V_{-1}$ . Then

$$\psi(x) = \sum_{n=-\infty}^{\infty} (-1)^n c_{-n+1} \phi(2x - n) \quad (16)$$

and its integer translates form an orthonormal basis for  $W_0$ . So  $\{\psi_{ij}(x) = 2^{i/2} \psi(2^i x - j), i, j \in \mathbb{Z}\}$  constitutes an orthonormal basis for  $L^2(\mathbb{R})$ , following (11). The implication of (15) is given graphically in Fig. 7 where it is shown how a scaling function can be obtained from a linear combination of its scaled versions. The first example is for illustration purposes only, while the second is an actual scaling function from a wavelet basis.

### C. The Discrete Time Case

Assume now that we deal with discrete time sequences  $x(n)$ ,  $n \in \mathbb{Z}$  which are square summable; that is, the space  $l^2(\mathbb{Z})$ . Now, let us derive a coarse half-resolution approximation to the original sequence. This can be done by filtering with a halfband low-pass filter, followed by subsampling by 2 (discarding every odd-indexed sample). In matrix notation, and assuming for the sake of simplicity that the filter is FIR, the convolution with a filter having impulse response  $[h_0(0), h_0(1), \dots, h_0(L-1)]$  followed by subsampling by 2, corresponds to matrix multiplication of the infinite signal vector  $x[\dots x(-1), x(0), x(1), \dots]$  by

$$\mathbf{H}_0 = \begin{bmatrix} \vdots & \vdots \\ \vdots & \vdots \\ \vdots & h_0(L-1) & h_0(L-2) & \cdots & \cdots & h_0(0) & 0 & 0 & \ddots \\ \vdots & 0 & 0 & h_0(L-1) & \cdots & h_0(2) & h_0(1) & h_0(0) & \vdots \\ \vdots & \vdots \\ \vdots & \vdots \end{bmatrix}. \quad (17)$$

Assume further that the impulse response and its shifted versions by even shifts (i.e., the rows of the above matrix) form an orthonormal set, that is,

$$\langle h_0(n-2l), h_0(n-2k) \rangle = \delta_{kl} \quad k, l \in \mathbb{Z}. \quad (18)$$

In matrix notation the equivalent of (18) is

$$\mathbf{H}_0 \mathbf{H}_0^* = \mathbf{I}.$$

The projection of the original sequence  $x(n)$  onto the sub-

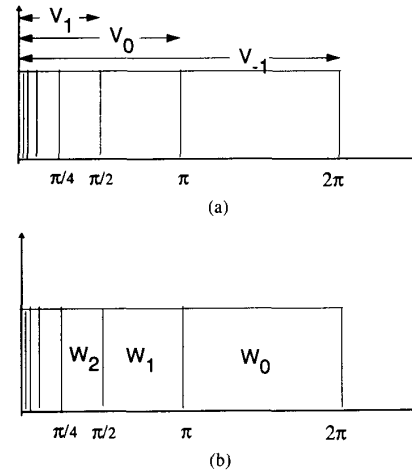


Fig. 5. Ideal division of spectrum using sinc filters. (a) Division into  $V_i$  spaces. Note that  $V_i \subset V_{i-1}$ . (b) Division into  $W_i$  spaces.

space spanned by the rows of  $\mathbf{H}_0$  is given by

$$\mathbf{H}_0^* \mathbf{H}_0 \cdot x.$$

Note that multiplication by  $\mathbf{H}_0^*$  corresponds to upsampling by 2 followed by convolution with a filter having impulse response  $\tilde{h}_0(n) = [h_0(L-1), h_0(L-2), \dots, h_0(1), h_0(0)]$ , (that is the time reversed impulse response of  $h_0(n)$ ). Note also that in order for the set  $\{h_0(n-2k), k \in \mathbb{Z}\}$  to form an orthonormal basis  $L$  has to be even. For if  $L$  were odd, then  $\langle h_0(n), h_0(n-L+1) \rangle = h_0(0)h_0(L-1) \neq 0$  unless either  $h_0(0)$  or  $h_0(L-1)$  is zero.

Call  $V_{-1}$  the space  $l^2(\mathbb{Z})$  and call  $V_0$  the subspace of  $V_{-1}$  spanned by the rows of  $\mathbf{H}_0$ . Then call  $W_0$  the orthogonal complement of  $V_0$  in  $V_{-1}$ :

$$V_{-1} = V_0 \oplus W_0.$$

Now the filter with impulse response  $h_1(n) = (-1)^n h_0(L-1-n)$  and its even shifted versions form an orthonormal basis for  $W_0$ . First note that orthogonality of  $h_0(n)$  and  $h_1(n)$  with respect to even shifts is easily veri-

fied, because of the sign change in  $h_1(n)$ :

$$\langle h_1(n-2l), h_0(n-2k) \rangle = 0 \quad k, l \in \mathbb{Z}. \quad (19)$$

In matrix notation calling  $\mathbf{H}_1$  a matrix based on  $h_1(n)$  in the same way that  $\mathbf{H}_0$  in (17) was based on  $h_0(n)$  we have

$$\mathbf{H}_0 \mathbf{H}_1^* = \mathbf{0}$$

thus  $V_0 \perp W_0$ . Then from the orthonormality of

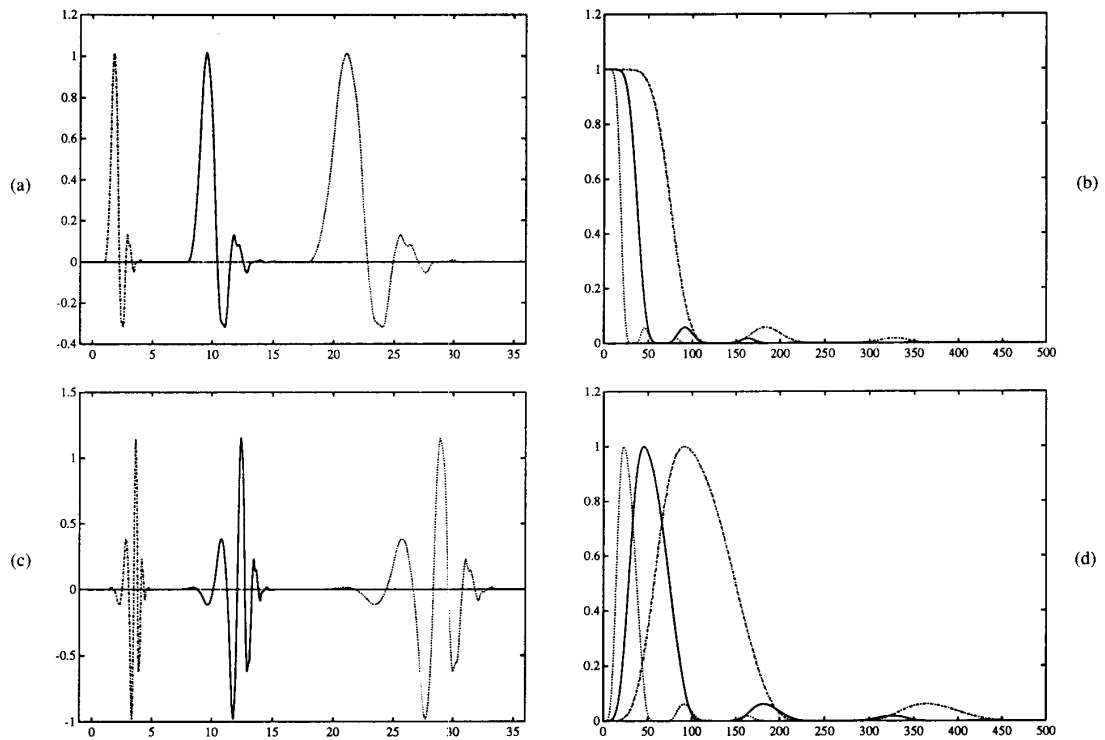


Fig. 6. Division of spectrum with a real wavelet. (a) Dyadic stretches of the scaling function. (b) Fourier transform of the stretched scaling functions, indicating the nesting of the  $V_j$  spaces. (c) Dyadic stretches of the wavelet. (d) Fourier transform of the stretched wavelets, indicating the arrangement of the  $W_j$  spaces.

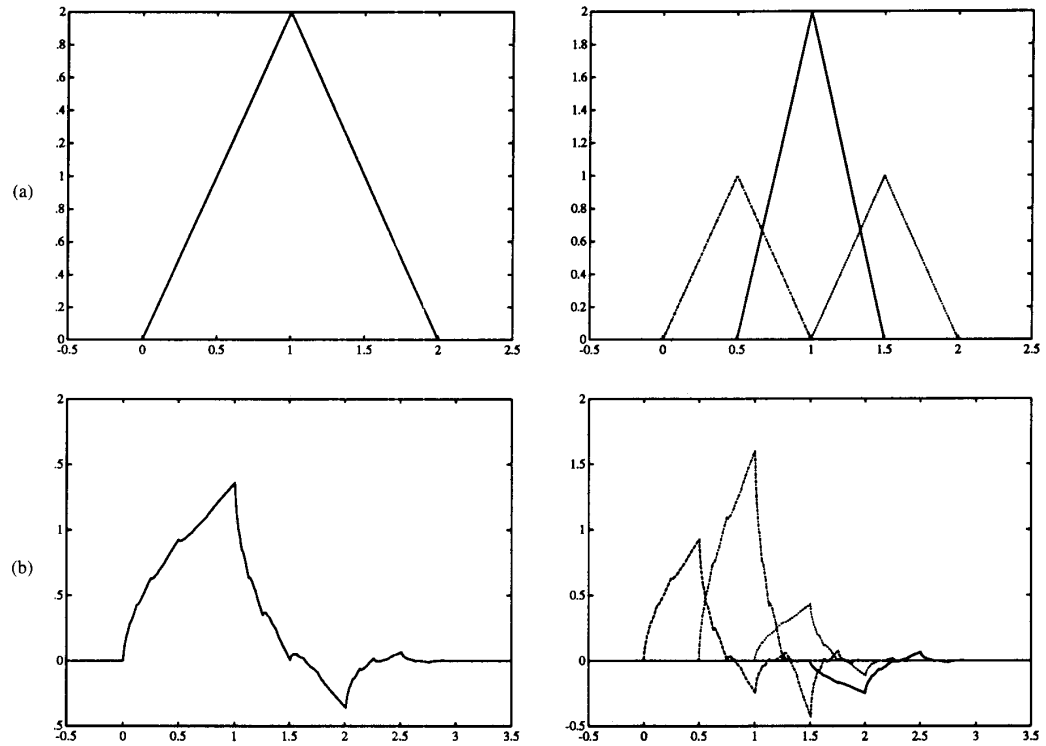


Fig. 7. Scaling function  $\phi(x)$  as a linear combination of scaled and shifted versions  $\phi(2x - n)$ . (a) Hat function example (this is not an orthonormal example). (b) Example based on a regular orthogonal 4-tap filter from [12].

$h_0(n - 2l)$  it follows

$$\langle h_1(n - 2l), h_1(n - 2k) \rangle = \delta_{kl} \quad k, l \in Z$$

since the sign change in  $h_1(n)$  is cancelled. In other words, based on an orthonormal basis for  $V_0$ , we were able to construct one for  $W_0$ , just as in the continuous case. Again in matrix notation

$$\mathbf{H}_1 \mathbf{H}_1^* = \mathbf{I} \quad (20)$$

and the projection of the original sequence onto  $W_0$  is given by

$$\mathbf{H}_1^* \mathbf{H}_1 \cdot \mathbf{x}.$$

Note that since we have projections onto orthonormal and complete subspaces:

$$\mathbf{H}_0^* \mathbf{H}_0 + \mathbf{H}_1^* \mathbf{H}_1 = \mathbf{I}.$$

It is also clear that by interleaving  $\mathbf{H}_0$  and  $\mathbf{H}_1$ , we obtain a block Toeplitz orthonormal matrix  $\mathbf{T}$ :

$$\mathbf{T} = \begin{bmatrix} \vdots & \vdots \\ h_0(L-1) & h_0(L-2) & \cdots & \cdots & h_0(0) & 0 & 0 & \vdots \\ h_1(L-1) & h_1(L-2) & \cdots & \cdots & h_1(0) & 0 & 0 & \vdots \\ \vdots & \vdots \\ 0 & 0 & h_0(L-1) & \cdots & h_0(2) & h_0(1) & h_0(0) & \vdots \\ 0 & 0 & h_1(L-1) & \cdots & h_1(2) & h_1(1) & h_1(0) & \vdots \\ \vdots & \vdots \end{bmatrix}.$$

which satisfies

$$\mathbf{T}\mathbf{T}^* = \mathbf{T}^*\mathbf{T} = \mathbf{I}$$

that is, the two filter impulse responses  $h_0(n)$  and  $h_1(n)$ , together with their even translates, form an orthonormal basis for  $l^2(Z)$ . Because this is such a fundamental concept we will illustrate it with an example. Instead of the rather trivial case where  $h_0(n) = 1/\sqrt{2} \cdot [1, 1]$  and  $h_1(n) = 1/\sqrt{2} \cdot [1, -1]$  (which corresponds to the Walsh-Hadamard transform on successive blocks of 2 samples), we will choose  $h_0(n) = [a_0 a_1, a_0 b_1, b_0 b_1, -b_0 a_1]$  where  $a_i = \cos \alpha_i$  and  $b_i = \sin \alpha_i$ . Because  $a_i^2 + b_i^2 = 1$  it is clear that  $\|h_0(n)\|_2 = 1$ . Also  $\langle h_0(n+2), h_0(n) \rangle = 0$  and thus  $h_0(n)$  and its even translates form an orthonormal set. Now choosing  $h_1(n) = [b_0 a_1, b_0 b_1, -a_0 b_1, a_0 a_1]$  makes  $h_1(n+2l)$  orthogonal to  $h_0(n)$  while keeping it of norm 1, and orthogonal to its even translates. Thus the set  $\{h_0(n+2l), h_1(n+2k); l, k \in Z\}$  is an orthonormal basis for  $l^2(Z)$ .

In Fig. 8, we recapitulate the above relations in the usual digital signal processing notation, using filters and sampling rate changes to denote the operators used so far. First the inner products  $\mathbf{H}_0 \cdot \mathbf{x}$  and  $\mathbf{H}_1 \cdot \mathbf{x}$  are calculated. Then the projections onto  $V_0$  and  $W_0$  are found. Finally, the original signal is reconstructed by adding the projections from the two orthogonal subspaces.

What worked once will work again; that is we can de-

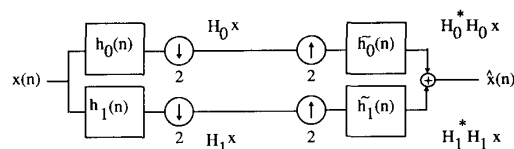


Fig. 8. Decomposition of  $V_{-1}$  into  $V_0$  and  $W_0$  using multirate filters, and recombination to achieve perfect reconstruction.  $\mathbf{H}_0^* \mathbf{H}_0 \cdot \mathbf{x}$  is the projection of the signal  $\mathbf{x}$  onto  $V_0$ , and  $\mathbf{H}_1^* \mathbf{H}_1 \cdot \mathbf{x}$  is the projection onto  $W_0$ .

compose  $V_0$  into  $V_1$  and  $W_1$  and so on. Hence we find

$$V_j \subset V_{j-1} \quad j = 0, 1, \dots$$

$$V_{j-1} = V_j \oplus W_j \quad j = 0, 1, \dots$$

from which we have

$$\dots V_2 \subset V_1 \subset V_0 \subset V_{-1}$$

and

$$V_{-1} = W_0 \oplus W_1 \oplus W_2 \oplus \dots$$

That is, the direct sum of all the  $W_i$ 's is the space of square summable functions  $l^2(Z)$ . Note that in contrast to the continuous case there is a "maximum" resolution in the discrete case given by  $V_{-1}$ , which is determined by the original sampling rate.

The decomposition of  $V_{-1}$  into  $W_0, W_1, W_2$ , etc, is essentially a wavelet transform on discrete sequences, since it splits the original space in two, and then splits one of the resulting half spaces in two, etc. This is shown in Fig. 9 using filters and subsamplers. Actually, if the filter  $h_0(n)$  is the ideal halfband low-pass filter given by (12), then  $h_1(n)$  is the ideal halfband high-pass filter. Thus if  $V_{-1}$  is the space of functions band limited to  $(-2\pi, 2\pi)$  as considered in the discussion of multiresolution analysis in Section II-B, then  $V_0$  and  $W_0$  are the spaces of functions band limited to  $(-\pi, \pi)$  and  $(-2\pi, -\pi) \cup (\pi, 2\pi)$ , respectively. That is, by iteration, the discrete system in Fig. 9 computes exactly the discrete wavelet transform into octave bands (although with noncausal infinite impulse response filters).

Note that the two concepts of scale and resolution introduced above, while related, are not the same. The notion of resolution of a signal is related to its bandwidth. This holds also in the sampled domain, but it is best thought of as the bandwidth of the equivalent continuous time signal. This definition indicates that an oversampled version will not have more resolution than a critically

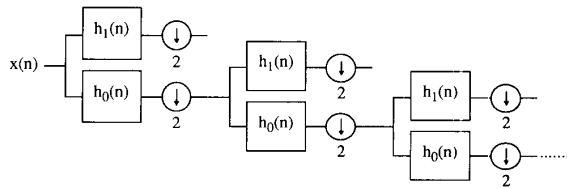


Fig. 9. Discrete wavelet transform on sequences. The halfband low-pass and high-pass filters are  $h_0(n)$  and  $h_1(n)$ , respectively, and  $\downarrow 2$  means subsampling by 2 (dropping samples with odd indexes).

sampled version of the same signal. The notion of scale is related to the size of a signal. We will adhere to the convention used in the wavelet literature, that large scale denotes contraction of the signal, while small scale stands for a dilated signal. Fig. 10 shows various multirate signal processing operations, and their effect upon resolution and scale (for simplicity only changes by factors of two are considered).

D. Orthogonal Pyramids and Critical Sampling

In computer vision and image coding [8], [9], a successive approximation or multiresolution technique called an image pyramid is sometimes used. It consists of deriving a low resolution version of the original, then predicting the original based on the coarse version, and finally taking the difference between the original and the prediction (see Fig. 11(a)). At the reconstruction, the prediction is added back to the difference, guaranteeing perfect reconstruction. A shortcoming of this scheme is the oversampling, since we end up with a low resolution version and a full resolution difference (at the initial rate). We briefly show below that, if the system is linear and the low-pass filter is orthogonal to its even translates, then one can actually subsample the difference signal after filtering it. In that case, the pyramid reduces exactly to a critically subsampled orthogonal subband coding scheme like the one discussed in the previous subsection.

First, the prediction of the original based on the coarse version is simply the projection onto the space spanned by  $\{h_0(-n - 2l), l \in \mathbb{Z}\}$ . That is, calling the prediction  $\bar{x}$ :

$$\bar{x} = H_0^* H_0 \cdot x.$$

The difference signal is thus

$$d = (I - H_0^* H_0) \cdot x.$$

But, because it is a perfect reconstruction system

$$I - H_0^* H_0 = H_1^* H_1$$

that is,  $d$  is the projection onto the space spanned by  $\{h_1(-n - 2l), l \in \mathbb{Z}\}$ . Therefore, we can filter and subsample  $d$  by 2, since, following (20)

$$H_1 H_1^* H_1 = H_1.$$

In that case, the redundancy of  $d$  is removed ( $d$  is now critically sampled), and the pyramid is equivalent to an orthogonal subband coding system (see Fig. 11(b)).

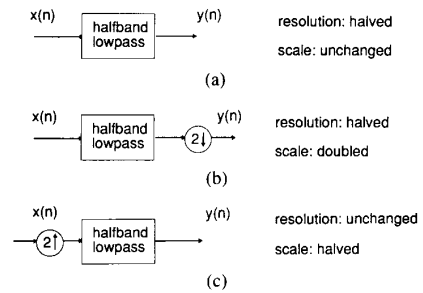


Fig. 10. Resolution and scale changes in discrete time (by factors of 2). Note that the scale of signals is defined as in geographical maps. (a) Halfband low-pass filtering reduces the resolution by 2 (scale is unchanged). (b) Halfband low-pass filtering followed by subsampling by 2 doubles the scale (and halves the resolution as in (a)). (c) Upsampling by 2 followed by halfband low-pass filtering halves the scale (resolution is unchanged).

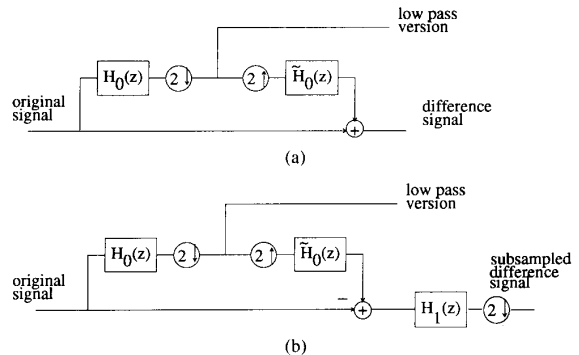


Fig. 11. Pyramid scheme involving a coarse low-pass approximation, and a difference between the coarse approximation and the original. (a) Oversampled case. (b) Critically sampled case, which is equivalent to a subband coding scheme.

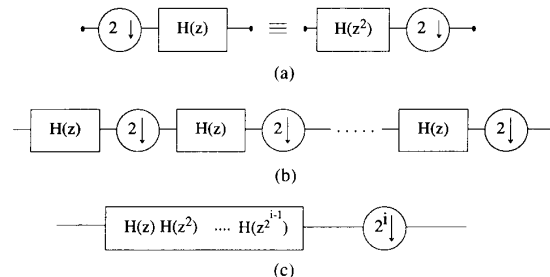


Fig. 12. Derivation of the equivalent iterated filter. (a) Subsampling by 2 before a filter  $H(z)$  can be written as filtering by  $H(z^2)$  followed by subsampling. (b) Cascade of  $i$  filters each followed by subsampling by 2. (c) Equivalent filter, followed by subsampling by  $2^i$ .

The signal  $d$  can be reconstructed by upsampling by 2 and filtering with  $\hat{h}_1(n)$ . Then we have

$$H_1^*(H_1 H_1^* H_1) \cdot x = H_1^* H_1 \cdot x = d$$

and this, added to  $\bar{x} = H_0^* H_0 \cdot x$  is indeed equal to  $x$ . In the notation of the multiresolution scheme described in Section II-C the prediction  $\bar{x}$  is the projection onto the space  $V_0$ , and  $d$  is the projection onto  $W_0$ . We have thus

shown that pyramidal schemes can be critically sampled as well. A similar analysis is given in [29]. It is interesting to note that although pyramid coding schemes have been in use for a decade or so, it had not been previously noted that they could be subsampled under the conditions above. The discussion of the more general, biorthogonal case (see also Section III-C) is given in Appendix A.1 and [24].

#### E. FIR Filter Banks and Compactly Supported Wavelets

We now briefly show the connection between wavelets of finite length and filter banks, as originally investigated by Daubechies [12]. Note that it is common to use the term compact support instead of finite length. First, assume we have an orthonormal basis of such functions  $\phi(x)$  and  $\psi(x)$  which obey two-scale difference equations as in (15) and (16):

$$\langle \phi(x+l), \phi(x+k) \rangle = \delta_{kl} \quad (21)$$

$$\langle \psi(x+l), \psi(x+k) \rangle = \delta_{kl} \quad (22)$$

$$\langle \phi(x+l), \psi(x+k) \rangle = 0. \quad (23)$$

We will show these relations lead to a perfect reconstruction FIR filter bank. The finite support of  $\phi(x)$  means that it can be written as a finite linear combination of the terms  $\phi(2x-n)$ ; that is, finitely many of the  $c_n$  are different from zero. From (21) we get

$$\langle \phi(2x-l), \phi(2x-k) \rangle = \frac{1}{2} \delta_{kl}. \quad (24)$$

Now, using (15) and (24), (21) can be written as (with  $n' = n - 2l$ , and  $m' = m - 2k$ ):

$$\begin{aligned} \langle \phi(x+l), \phi(x+k) \rangle &= \left\langle \sum_n c_n \phi(2x+2l-n), \sum_m c_m \phi(2x+2k-m) \right\rangle \\ &= \left\langle \sum_{n'} c_{n'+2l} \phi(2x-n'), \sum_{m'} c_{m'+2k} \phi(2x-m') \right\rangle \\ &= \frac{1}{2} \sum_{n'} c_{n'+2l} c_{n'+2k} = \delta_{kl} \end{aligned} \quad (25)$$

from which it follows that  $\|c_n\| = \sqrt{2}$ .

In other words the discrete filter, with impulse response  $h_0(n) = c_n/\sqrt{2}$  is orthogonal to its even translates, and with  $h_1(n) = (-1)^n h_0(L-n-1)$  we obtain an orthogonal perfect reconstruction FIR filter bank with orthogonal impulse responses. Thus, compactly supported wavelet bases lead to perfect reconstruction FIR filter banks. While the converse does not always hold, and is not as immediate to analyze, we discuss it here because it is the basis for the construction of compactly supported wavelets [12]. Considering the discrete time wavelet transform in Fig. 9, one notices that the lower branch is an infinite cascade of filters  $h_0(n)$  followed by subsampling by 2. Note that subsampling the signal with  $z$ -transform  $X(z)$  by 2 results in a new signal with  $z$ -transform  $Y(z)$ :

$$Y(z) = 1/2 \cdot [X(z^{1/2}) + X(-z^{1/2})] \quad (26)$$

It is easily verified that subsampling by 2 followed by fil-

tering with  $H(z)$  is equivalent to filtering with  $H(z^2)$  followed by subsampling by 2 (see Fig. 12(a)).

Therefore the cascade of  $i$  blocks of filtering operations followed by subsampling by 2 is equivalent to a filter  $H^{(i)}(z)$  with  $z$  transform:

$$H^{(i)}(z) = \prod_{l=0}^{i-1} H(z^{2^l}) \quad i = 1, 2, \dots \quad (27)$$

followed by subsampling by  $2^i$ . We define  $H^{(0)}(z) = 1$ . Assuming that the filter  $H(z)$  has an impulse response of length  $L$ , the length of the filter  $H^{(i)}(z)$  is  $L^{(i)} = (2^i - 1)(L - 1) + 1$  as can be checked from (27). Of course as  $i \rightarrow \infty$  we get  $L^{(i)} \rightarrow \infty$ . Now instead of considering the discrete time filter, we are going to consider the function  $f^{(i)}(x)$  which is piecewise constant on intervals of length  $1/2^i$ , and equal to

$$f^{(i)}(x) = 2^{i/2} \cdot h^{(i)}(n) \quad n/2^i \leq x < (n+1)/2^i. \quad (28)$$

Clearly,  $f^{(i)}(x)$  is supported on the interval  $[0, L-1]$ . Note that the normalization by  $2^{i/2}$  ensures that if  $\sum (h^{(i)}(n))^2 = 1$  then  $\int (f^{(i)}(x))^2 dx = 1$  as well. Also, it can be checked that  $\|h^{(i)}\|_2 = 1$  when  $\|h^{(i-1)}\|_2 = 1$ . A fundamental question is to find out whether and to what the function  $f^{(i)}(x)$  converges as  $i \rightarrow \infty$ . Fig. 13 shows two examples of such iterations. In Fig. 13(a) the first six iterates of the filter with impulse response  $[1, 3, 3, 1]$  show that it converges rapidly to a continuous function; while in Fig. 13(b) the iterates of the filter  $[-1, 3, 3, -1]$  tend to a discontinuous function. In other words, different filters exhibit very different behavior. Of course when constructing wavelets of compact support one would like them to be continuous functions, perhaps possessing continuous derivatives also. This can be achieved if the filter meets certain regularity constraints; so that the limit function  $f^{(\infty)}(x)$  is continuous. In [12] Daubechies gives such a condition, which we now review.

First, assume that the filter  $H(z)$  has a zero at the half sampling frequency, or  $H(e^{j\pi}) = 0$ . This is not unreasonable since  $H(z)$  is to be a halfband low-pass filter; in fact if  $f^{(i)}(x)$ ,  $i \rightarrow \infty$  is to converge to a continuous function at least one such zero is necessary [34], [35]. This together with the fact that the filter impulse response is orthogonal to its even translates is equivalent to  $\sum h(n) = H(1) = \sqrt{2}$ . Define  $m_0(z) = 1/\sqrt{2} \cdot H(z)$ , that is  $m_0(1) = 1$ . Now factor  $m_0(z)$  into its roots at  $\pi$  (there is at least one by assumption) and a remainder polynomial  $R(z)$ , in the following way:

$$m_0(z) = [(1+z^{-1})/2]^N R(z).$$

Note that  $R(1) = 1$  from the definitions. Now call  $B$  the supremum of  $|R(z)|$  on the unit circle:

$$B = \sup_{\omega \in [0, 2\pi]} |R(e^{j\omega})|.$$

Then the following result from [12] holds.

**Proposition 2.1 [12]:** *If  $B < 2^{N-1}$ , then the piecewise constant function  $f^{(i)}(x)$  defined in (28) converges pointwise to a continuous function  $f^{(\infty)}(x)$ .*

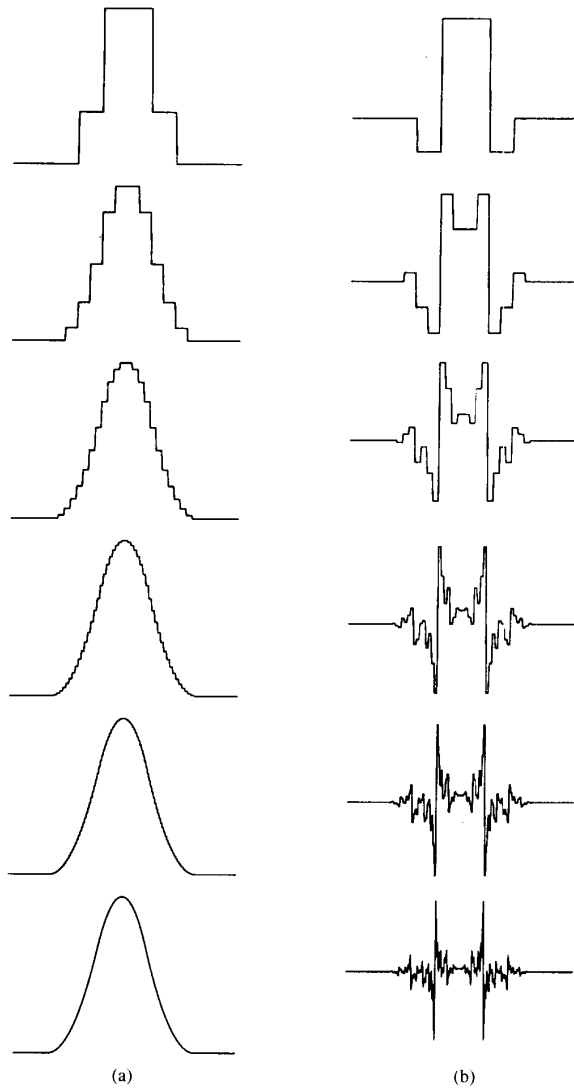


Fig. 13. Iteration (28) for two simple filters. (a) [1, 3, 3, 1] which converges to a continuous function. (b) [-1, 3, 3, -1] which converges to a discontinuous function.

This is a sufficient condition to ensure pointwise convergence to a continuous function, and can be used as a simple test. Note that more accurate methods are available for testing regularity [36], [12], [35]. The reason for our interest in this bound is that we can make it a design criterion to place a maximum number of zeros at  $\pi$ . This approach is explored in Section V-A.

Various methods for estimating the regularity index  $\beta$  such that  $\psi(x), \phi(x) \in C^\beta$  are available [12], [35]. We shall use the methods of [35] to check the limit functions that we design. These are especially useful if a filter fails the test of proposition 2.1.

Note that if  $m_0(z)$  has a zero of order  $N$  at  $z = -1$  then the wavelet generated will have  $N$  consecutive vanishing moments. That is  $\int x^k \psi(x) dx = 0, k = 0, 1, \dots, N -$

1, [12]. This property is potentially useful for the compression of smooth functions by wavelet transforms.

### F. Bases of Orthonormal Wavelets Constructed from Filter Banks

Finally, we show that if the filter used in (27) exhibits the orthogonality with respect to even shifts described in Section II-C, and is regular (for example, if it meets the conditions of proposition 2.1) then the infinitely iterated filter bank generates orthogonal sets of wavelets. That is, if filters  $h_0(n)$  and  $h_1(n)$  and their even translates form an orthonormal set in  $l^2(\mathbb{Z})$ , then we generate functions  $\phi(x), \psi(x)$ , which together with their integer translates, form an orthonormal set in  $L^2(\mathbb{R})$ . These relations are derived in [12]; we rederive them since we shall use similar reasoning later in the biorthogonal case (Section III-D).

First, using (27) and (28)

$$f^{(i)}(x) = 2^{i/2} \cdot \sum_{m=0}^{L-1} h_0(m) \cdot h_0^{(i-1)}(n - 2^{i-1}m) \quad (29)$$

$$n/2^i \leq x < (n+1)/2^i$$

To write  $h_0^{(i-1)}(n - 2^{i-1}m)$  in terms of  $f^{(i-1)}(x)$  observe

$$f^{(i-1)}(2x - m) = 2^{(i-1)/2} \cdot h_0^{(i-1)}(n) \quad (30)$$

$$n/2^{i-1} \leq 2x - m < (n+1)/2^{i-1}$$

that is, we have an expression for  $f^{(i-1)}(2x - m)$  when  $x$  is in the interval  $[(n + 2^{i-1}m)/2^i, (n + 2^{i-1}m + 1)/2^i]$ . Making the change of variable:  $n' = n + 2^{i-1}m$  this gives

$$f^{(i)}(x) = 2^{1/2} \cdot \sum_{m=0}^{L-1} h_0(m) \cdot f^{(i-1)}(2x - m). \quad (31)$$

Recall that when the filter is regular,  $f^{(i)}(x)$  tends to a continuous limit function  $\phi(x)$  as  $i \rightarrow \infty$ . By taking the limit in (31),  $\phi(x)$  itself satisfies a two-scale difference equation:

$$\phi(x) = 2^{1/2} \cdot \sum_{n=0}^{L-1} h_0(n) \cdot \phi(2x - n). \quad (32)$$

We can define also the bandpass function:

$$\psi(x) = 2^{1/2} \cdot \sum_{n=0}^{L-1} h_1(n) \cdot \phi(2x - n). \quad (33)$$

Assume now that we have filters such that the impulse responses are orthogonal with respect to even shifts:

$$\langle h_i(n - 2l), h_j(n - 2k) \rangle = \delta_{ij} \delta_{kl} \quad k, l \in \mathbb{Z}. \quad (34)$$

We show now that  $\phi(x)$  is orthogonal to integer translates of itself  $\forall i$ . From the definition (28)  $f^{(0)}(x)$  is just the indicator function on the interval  $[0, 1)$ ; so we immediately get orthogonality at the 0th level, that is,  $\langle f^{(0)}(x - l), f^{(0)}(x - k) \rangle = \delta_{kl}$ . Now we assume orthogonality at the  $i$ th level:

$$\langle f^{(i)}(x - l), f^{(i)}(x - k) \rangle = \delta_{kl} \quad (35)$$

and prove that this implies orthogonality at the  $(i + 1)$ st level:

$$\begin{aligned} & \langle f^{(i+1)}(x - l), f^{(i+1)}(x - k) \rangle \\ &= 2 \sum_n \sum_m h_0(n)h_0(m) \langle f^{(i)}(2x - 2l - n), \\ & \quad f^{(i)}(2x - 2k - m) \rangle \\ &= \sum_n h_0(n)h_0(n + 2l - 2k) \\ &= \delta_{kl}. \end{aligned}$$

Hence, by induction (35) holds for all  $i$ . So in the limit  $i \rightarrow \infty$ :

$$\langle \phi(x - l), \phi(x - k) \rangle = \delta_{kl}. \quad (36)$$

The other orthogonality relations between  $\psi(x)$  and  $\phi(x)$  now follow easily from (34):

$$\begin{aligned} \langle \psi(x - l), \psi(x - k) \rangle &= \delta_{kl} \\ \langle \phi(x - l), \psi(x - k) \rangle &= 0. \end{aligned} \quad (37)$$

To end the section we show that  $\psi(x)$  is orthogonal across scale. First, across one scale:

$$\begin{aligned} & \langle \psi(x - l), \psi(2x - k) \rangle \\ &= \left\langle \sum_n h_1(n) \cdot \phi(2x - 2l + n), \psi(2x - k) \right\rangle \\ &= \sum_n h_1(n) \langle \phi(2x - 2l + n), \psi(2x - k) \rangle \\ &= 0. \end{aligned}$$

Similar reasoning shows that across several scales  $\psi(2^j x - l)$  is orthogonal to  $\psi(2^j x - k)$  for  $j \neq i$  and  $k \neq l$ . We have shown the correspondence between the orthogonality relations of the filter impulse responses, and those of their infinite iterates. Besides orthogonality, completeness is required in order that  $\{2^{-j/2}\psi(2^j x - l), j, l \in \mathbb{Z}\}$  be an orthonormal basis for  $L^2(\mathbb{R})$ , and this is proved in [12]. Thus any function  $f(x) \in L^2(\mathbb{R})$  can be written as

$$f(x) = \sum_j \sum_l \langle 2^{-j/2}\psi(2^j x - l), f(x) \rangle 2^{-j/2}\psi(2^j x - l).$$

### III. GENERAL FIR PERFECT RECONSTRUCTION FILTER BANKS AND BIORTHOGONAL WAVELETS

Since we will be using perfect reconstruction filter banks (PRFB's) to construct wavelets, we briefly review the salient points here. For greater detail, we refer for example to [19]–[22]. Assume that we have a filter bank as in Fig. 8, with analysis filters  $H_0(z)$  and  $H_1(z)$  but with general synthesis filters  $G_0(z)$  and  $G_1(z)$  instead of  $\tilde{H}_0(z)$  and  $\tilde{H}_1(z)$ . Note that upsampling by 2 (inserting a zero between every two samples) corresponds to simply replacing  $z$  by  $z^2$  in the  $z$  transform. Using (26) it is easily seen that the output of the analysis/synthesis system is

given by

$$\hat{X}(z) = \frac{1}{2} [G_0(z) \ G_1(z)] \cdot \begin{bmatrix} H_0(z) & H_0(-z) \\ H_1(z) & H_1(-z) \end{bmatrix} \begin{bmatrix} X(z) \\ X(-z) \end{bmatrix}. \quad (38)$$

Call the above  $2 \times 2$  matrix  $\mathbf{H}_m(z)$ , where the subscript  $m$  indicates that it contains modulated versions of the filters  $H_0(z)$  and  $H_1(z)$ . Note that from the above equation in order to eliminate the contribution to the reconstructed signal from  $X(-z)$  (which represents an aliased version of the signal) it is necessary and sufficient that the synthesis filters are related to the analysis filters as follows:

$$[G_0(z), G_1(z)] = C(z) [H_1(-z), -H_0(-z)]. \quad (39)$$

Note that

$$\det [\mathbf{H}_m(z)] = H_0(z)H_1(-z) - H_0(-z)H_1(z) \quad (40)$$

$$= P(z) - P(-z) \quad (41)$$

where  $P(z) = H_0(z)H_1(-z)$ . We introduce the following polyphase notation for the filters:

$$H_i(z) = H_{i0}(z^2) + z^{-1}H_{i1}(z^2)$$

that is,  $H_{i0}(z)$  contains the even-indexed coefficients of the filter  $H_i(z)$ , while  $H_{i1}(z)$  contains the odd ones. Thus

$$\begin{bmatrix} H_{00}(z^2) & H_{01}(z^2) \\ H_{10}(z^2) & H_{11}(z^2) \end{bmatrix} = \frac{1}{2} \begin{bmatrix} H_0(z) & H_0(-z) \\ H_1(z) & H_1(-z) \end{bmatrix} \begin{bmatrix} 1 & 1 \\ 1 & -1 \end{bmatrix} \begin{bmatrix} 1 & 0 \\ 0 & z \end{bmatrix}$$

or

$$\mathbf{H}_p(z^2) = 2^{-1} \cdot \mathbf{H}_m(z) \begin{bmatrix} 1 & 1 \\ 1 & -1 \end{bmatrix} \begin{bmatrix} 1 & 0 \\ 0 & z \end{bmatrix}$$

where  $\mathbf{H}_p(z)$  is called the polyphase matrix. In particular,

$$\det [\mathbf{H}_m(z)] = -2z^{-1} \det [\mathbf{H}_p(z^2)] \quad (42)$$

and

$$\begin{aligned} \det [\mathbf{H}_p(z)] &= H_{00}(z)H_{11}(z) - H_{01}(z)H_{10}(z) \\ &= 1/2 \cdot z^{1/2} [P(z^{1/2}) - P(-z^{1/2})]. \end{aligned} \quad (43)$$

#### A. FIR Filter Banks

For convenience we repeat the following well-known fact [37], [38], [21].

*Fact 3.1: For perfect reconstruction with FIR synthesis filters after an FIR analysis, it is necessary and sufficient that*

$$\det [\mathbf{H}_m(z)] = c \cdot z^{-2l-1} \quad \text{where } l \in \mathbb{Z}.$$

Note that  $\det [\mathbf{H}_p(z)]$  is thus a pure delay as well. In order to make the results that follow less arbitrary, we shall fix  $c = 2$ . This involves no loss of generality, since filters that differ only by a multiplicative constant can be regarded as equivalent.

From this, and (40) it follows that  $P(z)$  can have only

a single nonzero odd-indexed coefficient:

$$P(z) - P(-z) = 2p_{2l+1}z^{-2l-1} \quad (44)$$

and we would normalize  $p_{2l+1} = 1$ . A polynomial  $P(z)$  satisfying this constraint is termed a *valid* polynomial. It is then clear that any factorization of a valid  $P(z) = H_0(z)H_1(-z)$  gives a possible FIR PRFB. Note that  $H_0(z)$  and  $H_1(-z)$  are interchangeable. Given an FIR filter  $H_0(z)$  we use the term complementary filter to denote any  $H_1(z)$  such that  $P(z) = H_0(z)H_1(-z)$  is a valid polynomial; that is  $H_0(z)$  and  $H_1(z)$  form a PR filter pair.

The above discussion indicates two possible design methods for PRFB's [21]. First the factorization method consists of finding a valid  $P(z)$  satisfying design criteria, and then factoring it into  $H_0(z)$  and  $H_1(-z)$ . Second, the complementary filter method starts with a filter  $H_0(z)$  and then solves a system of linear equations to find a complementary filter leading to a valid  $P(z)$ . (Note that this  $P(z)$  can then be refactored as desired.) Of course once we have designed  $P(z)$  and factored it in terms of the analysis filters  $H_0(z)$  and  $H_1(-z)$  the synthesis filters follow directly from (39), with  $C(z) = c \cdot z^{-l}$ .

### B. Orthogonal or Paraunitary Filter Banks

In Section III-C we have seen how to construct unitary operators based on filters which were orthogonal to their even translates. In filtering notation this means that the even terms of the autocorrelation function are all zero, with the exception of the central one (which equals unity for normalized filters). The autocorrelation of a filter  $H_i(z)$  is  $H_i(z)H_i(z^{-1})$ ; thus the condition (18) becomes

$$H_i(z)H_i(z^{-1}) + H_i(-z)H_i(-z^{-1}) = 2 \quad i \in \{0, 1\}. \quad (45)$$

Further, the two filters  $H_0(z)$  and  $H_1(z)$  were orthogonal to each other at even translates (19), so the even terms of the cross correlation are all zero:

$$H_0(z)H_1(z^{-1}) + H_0(-z)H_1(-z^{-1}) = 0. \quad (46)$$

If the two filters satisfy (45) and (46), their impulse responses and even translates form an orthogonal basis for  $l^2(\mathbb{Z})$ . We are now ready to prove a fact on the form of orthogonal FIR solutions:

*Fact 3.2: Consider an FIR perfect reconstruction filter bank such that  $H_0(z)$  satisfies (45). Then the length of  $h_0(n)$  has to be even. In order that  $h_0(n - 2k)$  and  $h_1(n - 2l)$  form an orthogonal basis (that is  $H_1(z)$  should satisfy (45) and (46)), it is necessary and sufficient that*

$$H_1(z) = z^{-2k-1}H_0(-z^{-1}). \quad (47)$$

*Proof:* That  $L$  must be even was already shown in Section II-C. That a complementary filter given by (47) satisfies (45) and (46) and leads to perfect reconstruction is easily verified by substitution.

Necessity is shown as follows: from (46) it is known that  $H_0(z)H_1(z^{-1})$  is a polynomial with only odd coeffi-

cients, that is

$$H_0(z)H_1(z^{-1}) = z^{-2n-1}Q(z^2).$$

So the zeros appear in pairs at  $(\alpha, -\alpha)$ . Proposition 4.3 below states that  $H_0(z)$  cannot have such a pair of zeros if PR is to be possible; thus for every zero at  $z = \alpha$  in  $H_0(z)$ , there must be a corresponding zero at  $z = -\alpha$  in  $H_1(z^{-1})$ . This means that  $H_1(z)$  has a zero at  $z = -1/\alpha$ ; so  $H_1(z)$  has the form given in (47).  $\square$

This necessary form of  $H_1(z)$  means that

$$H_1(z) = -z^{-2k}H_{01}(z^{-2}) + z^{-2k-1}H_{00}(z^{-2}).$$

Choosing  $k = 0$  leads to:

$$\mathbf{H}_p(z) = \begin{bmatrix} H_{00}(z) & H_{01}(z) \\ -H_{01}(z^{-1}) & H_{00}(z^{-1}) \end{bmatrix}. \quad (48)$$

Because it is a perfect reconstruction system

$$\det[\mathbf{H}_p(z)] = H_{00}(z)H_{00}(z^{-1}) + H_{01}(z)H_{01}(z^{-1}) = 1 \quad (49)$$

since  $\det[\mathbf{H}_p(z)]$  has to be a delay, and is symmetric. This is the polyphase equivalent of (45), because the even coefficients of the autocorrelation  $H_0(z)H_0(z^{-1})$  are given by (49). On the unit circle  $z = e^{j\omega}$ , this means that

$$|H_{00}(e^{j\omega})|^2 + |H_{01}(e^{j\omega})|^2 = 1 \quad (50)$$

that is they form a power complementary pair [38].

The necessary form (47) also means that, substituting into (40)

$$z^{-2k-1}[H_0(z)H_0(z^{-1}) + H_0(-z)H_0(-z^{-1})] = 2z^{-2k-1}.$$

Or, on the unit circle

$$|H_0(e^{j\omega})|^2 + |H_0(e^{j(\omega+\pi)})|^2 = 2.$$

Note that the matrix  $\mathbf{H}_p(z)$  in (48) has the following property:

$$\begin{aligned} & [\mathbf{H}_p(z^{-1})]^T \cdot \mathbf{H}_p(z) \\ &= \begin{bmatrix} H_{00}(z^{-1}) & -H_{01}(z) \\ H_{01}(z^{-1}) & H_{00}(z) \end{bmatrix} \begin{bmatrix} H_{00}(z) & H_{01}(z) \\ -H_{01}(z^{-1}) & H_{00}(z^{-1}) \end{bmatrix} \\ &= \begin{bmatrix} 1 & 0 \\ 0 & 1 \end{bmatrix} \end{aligned}$$

because of (49). In other words, it is unitary on the unit circle; such a matrix is called a paraunitary matrix [38]; if it is also stable it is called lossless [39], [40]. This is the extension of the allpass filter concept [41] to matrices with polynomial entries.

The above discussion indicates two possible design approaches. The first is to find an autocorrelation function that has only a single even-indexed coefficient different from zero. This must be the central one, since an autocorrelation function is symmetric. Such a function can be factored into its "square roots"  $H_0(z)$  and  $H_0(z^{-1})$ . In particular, zeros on the unit circle have to be double, since

the function must not change sign. This method was first used by Smith and Barnwell [37] and Mintzer [18] to synthesize orthogonal filter banks. The second method uses lattice structures to synthesize paraunitary matrices, for which complete factorizations have been given by Vaidyanathan and Hoang [20].

Note that designs in the filter bank literature did not address the question of regularity (see proposition 2.1). Daubechies [12] specifically designed filters satisfying the above orthogonality relations and having a maximum number of zeros at  $\pi$ .

### C. Biorthogonal or General Perfect Reconstruction Filter Banks

From fact 3.1, we know that perfect reconstruction requires  $\det [\mathbf{H}_m(z)]$  to be an odd delay, and the synthesis filters are given by (39) with  $C(z) = c \cdot z^{-l}$ .

Choose  $l = 1$  for the purposes of this discussion. First note that  $G_0(z)H_1(z)$  and  $G_1(z)H_0(z)$  have only odd coefficients, that is,

$$\langle \bar{g}_0(n - 2k), h_1(n - 2l) \rangle = 0 \quad (51)$$

$$\langle \bar{g}_1(n - 2k), h_0(n - 2l) \rangle = 0 \quad (52)$$

(note the time reversal in the inner product). In matrix notation

$$\mathbf{H}_0 \mathbf{G}_1 = \mathbf{0} = \mathbf{H}_1 \mathbf{G}_0 \quad (53)$$

where  $\mathbf{H}_i$  and  $\mathbf{G}_i$  have been defined in a fashion similar to (17). Now  $G_0(z)H_0(z) = z^{-1}H_0(z)H_1(-z)$  has a single nonzero odd coefficient (because it is a PR system). Similarly  $G_1(z)H_1(z)$  has also only a single even-indexed coefficient different from zero. That is,

$$\langle \bar{g}_i(n - 2l), h_i(n) \rangle = \delta_i. \quad (54)$$

In operator notation

$$\mathbf{H}_0 \mathbf{G}_0 = \mathbf{I} = \mathbf{H}_1 \mathbf{G}_1. \quad (55)$$

Since we have a perfect reconstruction system, we get

$$\mathbf{G}_0 \mathbf{H}_0 + \mathbf{G}_1 \mathbf{H}_1 = \mathbf{I}. \quad (56)$$

Of course the last equation above indicates that no nonzero vector can lie in the column nullspaces of both  $\mathbf{H}_0$  and  $\mathbf{H}_1$ . Note that (55) implies that  $\mathbf{G}_0 \mathbf{H}_0$  and  $\mathbf{G}_1 \mathbf{H}_1$  are each projections (since  $\mathbf{G}_i \mathbf{H}_i \mathbf{G}_i \mathbf{H}_i = \mathbf{G}_i \mathbf{H}_i$ ). They project onto subspaces which are not in general orthogonal. Note that (51) and (52) indicate, however, that there are orthogonality relations between the filter impulse responses. Because of (51), (52), and (54) the analysis synthesis system is termed biorthogonal. In the special case where we have a paraunitary solution one finds:  $\mathbf{G}_0 = \mathbf{H}_0^*$  and  $\mathbf{G}_1 = \mathbf{H}_1^*$ , and (53) gives that we have projections onto subspaces which are mutually orthogonal. Further considerations on biorthogonal systems can be found in [28], [29].

One reason to use biorthogonal rather than orthogonal bases is that the additional freedom allows us to have arbitrary length linear phase filters. It is well known [12], [23], [22] that the only orthogonal (or paraunitary) real

FIR filter bank having linear phase has only two nonzero taps, and is given by  $H_0(z) = z^{-l} + z^{-l-2n-1}$  and  $H_1(z) = (z^{-l} - z^{-l-2n-1})z^{-2n}$ . (Note that paraunitary filters can be factorized so as to approximate linear phase [17], [42], [29].)

To obtain longer real FIR filters, and still have exact linear phase, one has to give up orthogonality. The classes of linear phase solutions are indicated below.

*Proposition 3.3: Linear phase perfect reconstruction real FIR filter banks using filters  $H_0(z)$  and  $H_1(z)$  have one of the following forms:*

a) Both filters are symmetric and of odd lengths, differing by an odd multiple of 2.

b) One filter is symmetric and the other is antisymmetric; both lengths are even, and are equal or differ by an even multiple of 2.

c) One filter is of odd length, the other is even; both have all zeros on the unit circle. Either both filters are symmetric, or one is symmetric and the other is antisymmetric.

*Proof:* See Appendix A.2.

In class c) we find that  $P(z) = H_0(z)H_1(-z)$  has zeros only at the  $2n - 1$  roots of  $\pm 1$ ; so the filters are of very little practical interest. We will not consider this trivial solution further.

It is also possible to get lattice structures that generate linear phase FIR filter banks [23], [22]. Appendix A.3 indicates the lattice that will generate the low-pass  $H_0(z) = (1 + z^{-1})^{2N}$  (that is the "most regular" low pass, following proposition 2.1) and its complementary filter  $H_1(z)$ . A general discussion of complementary filters in the biorthogonal case is given in Appendix A.3. The discussion of the biorthogonal pyramid is presented in Appendix A.1.

Note that while in the FIR case it is necessary to give up orthogonality to get nontrivial linear phase solutions, in the IIR case it is possible to have both; the filters are noncausal, but good designs are possible [25].

### D. Biorthogonal Wavelets Based on Filter Banks

To tie together the results of this section we now show that the infinitely iterated biorthogonal perfect reconstruction filter banks generate biorthogonal sets of functions.

We denote by  $H_0^{(i)}(z)$  and  $G_0^{(i)}(z)$  the filters which are equivalent to the cascade of  $i$  blocks of filtering/subsampling in the analysis and synthesis sections, respectively. We assume that both of the filters involved are regular. From these define functions which are piecewise constant on intervals of length  $1/2^i$ :

$$f^{(i)}(x) = 2^{i/2} \cdot h_0^{(i)}(n) \quad n/2^i \leq x < (n+1)/2^i \quad (57)$$

$$\tilde{f}^{(i)}(x) = 2^{i/2} \cdot \bar{g}_0^{(i)}(n) \quad n/2^i \leq x < (n+1)/2^i. \quad (58)$$

Note that we assume regularity, that is in the limit as  $i \rightarrow$

$\infty$  both  $f^{(i)}(x)$  and  $\check{f}^{(i)}(x)$  converge to continuous functions. Using the analysis in Section II-F we easily show that  $f^{(i)}(x)$  and  $\check{f}^{(i)}(x)$  lead to limit functions which satisfy the two-scale difference equations:

$$\phi(x) = 2^{1/2} \cdot \sum_{n=0}^{L-1} h_0(n) \cdot \phi(2x - n) \tag{59}$$

$$\check{\phi}(x) = 2^{1/2} \cdot \sum_{n=0}^{L-1} \check{g}_0(n) \cdot \check{\phi}(2x - n). \tag{60}$$

Define also the associated bandpass functions:

$$\psi(x) = 2^{1/2} \cdot \sum_{n=0}^{L-1} h_1(n) \cdot \phi(2x - n) \tag{61}$$

$$\check{\psi}(x) = 2^{1/2} \cdot \sum_{n=0}^{L-1} \check{g}_1(n) \cdot \check{\phi}(2x - n). \tag{62}$$

That  $\check{\phi}(x)$  and  $\phi(x)$  are orthogonal with respect to integer shifts is again shown inductively. We immediately get orthogonality at the 0th level since  $\check{f}^{(0)}(x)$  and  $f^{(0)}(x)$  are each equal to the indicator function on the interval  $[0, 1)$ :  $\langle \check{f}^{(0)}(x - 1), f^{(0)}(x - k) \rangle = \delta_{kl}$ . Again assume orthogonality at the  $l$ th level:  $\langle \check{f}^{(l)}(x - 1), f^{(l)}(x - k) \rangle = \delta_{kl}$ . And then get

$$\begin{aligned} &\langle \check{f}^{(i+1)}(x - 1), f^{(i+1)}(x - k) \rangle \\ &= 2 \left\langle \sum_n \check{g}_0(n) \cdot \check{f}^{(i)}(2x - 2k - n), \right. \\ &\quad \left. \sum_m h_0(m) f^{(i)}(2x - 2l - m) \right\rangle \\ &= \sum_n \check{g}_0(n) \cdot h_0(n + 2l - 2k) \\ &= \delta_{kl}. \end{aligned}$$

In the limit this gives

$$\langle \check{\phi}(x - l), \phi(x - k) \rangle = \delta_{kl}. \tag{63}$$

Once this is established

$$\langle \check{\psi}(x - l), \psi(x - k) \rangle = \delta_{kl} \tag{64}$$

follows immediately from (54); and the relations

$$\langle \check{\phi}(x - l), \psi(x - k) \rangle = 0 \tag{65}$$

$$\langle \check{\psi}(x - l), \phi(x - k) \rangle = 0 \tag{66}$$

come from (51) and (52), respectively.

We have shown that the conditions for perfect reconstruction on the filter coefficients lead to functions that have the biorthogonality properties as shown above. Orthogonality across scale is also verified, following the analysis of Section II-F:

$$\langle 2^{-j/2} \check{\psi}(2^j x - l), 2^{-i/2} \psi(2^i x - k) \rangle = \delta_{ij} \delta_{kl}.$$

Thus the set  $\{\psi(2^j x - l), \check{\psi}(2^i x - k), i, j, k, l \in \mathbb{Z}\}$  is biorthogonal. That it is complete can be verified as in the

orthogonal case [28]. Hence any function from  $L^2(\mathbb{R})$  can be written

$$f(x) = \sum_j \sum_l \langle 2^{-j/2} \psi(2^j x - l), f(x) \rangle 2^{-j/2} \check{\psi}(2^j x - l).$$

Note that  $\psi(x)$  and  $\check{\psi}(x)$  play interchangeable roles.

So, regular biorthogonal FIR filter banks lead to biorthogonal bases of functions of finite length; it is easily shown that the converse is also true. Assume that we have functions  $\psi(x), \phi(x), \check{\phi}(x), \check{\psi}(x)$  satisfying (59)–(62) and (63)–(66). Then it is easy to verify that they can be used to derive biorthogonal filter banks. For example, using (63)

$$\begin{aligned} &\langle \check{\phi}(x - l), \phi(x - k) \rangle \\ &= \left\langle \sum_n \check{g}_0(n) \cdot \check{\phi}(2x - 2l - n), \right. \\ &\quad \left. \sum_m h_0(m) \phi(2x - 2k - m) \right\rangle \\ &= \sum_n \sum_m \check{g}_0(n) \cdot h_0(m) \langle \check{\phi}(2x - 2l - n), \\ &\quad \phi(2x - 2k - m) \rangle \\ &= \sum_n \check{g}_0(n) \cdot h_0(n + 2l - 2k) = \delta_{kl}. \end{aligned}$$

The other filter biorthogonality relations follow from (64)–(66).

### E. Filter Design

Propositions 2.1 gives a sufficient condition to ensure pointwise convergence to a continuous function, which hinges on the number of zeros at  $\pi$ . It is clear that a filter with a maximum number of zeros at  $\pi$  will not necessarily be maximally regular. Ideally, to get a maximally regular filter (which is written  $H(z) = [(1 + z^{-1})/2]^N F(z)$  as in Section II-E) we would maximize  $N$  while simultaneously minimizing  $\sup_{\omega \in [0, 2\pi]} |F(e^{j\omega})|$ . There is a tradeoff involved. However only  $N$ , the number of zeros at  $\pi$ , can be easily controlled.

The question of regularity is more involved for the biorthogonal case than it is in the orthogonal case, since now we have to check the regularity of both the analysis ( $H_0(z)$ ) and synthesis ( $H_1(-z)$ ) low-pass filters (see Section V-A). Fig. 14 illustrates the difficulty of making both  $H_0(z)$  and  $H_1(-z)$  regular for the length 4 linear phase case. Recall that the impulse responses of  $H_0(z)$  and  $H_1(-z)$  are given by  $[1, \alpha, \alpha, 1]$  and  $[1, -\alpha, -\alpha, 1]$ , respectively [22]. The figure shows the scaling function generated by  $[1, \alpha, \alpha, 1]$  for  $\alpha \in [-3, 3]$ . At  $\alpha = 3$  we have that  $H_0(z)$  is very regular, while  $H_1(-z)$  is very irregular (as shown also in Fig. 13). The difference between the regularity of the two filters clearly decreases as  $\alpha$  gets smaller, without ever leading to two regular linear phase perfect reconstruction filters of length 4. Actually at  $\alpha = 0$  there is neither pointwise nor  $L^2$  convergence [12] (the figure which shows the sixth iteration gives therefore an erroneous impression at  $\alpha = 0$ ).

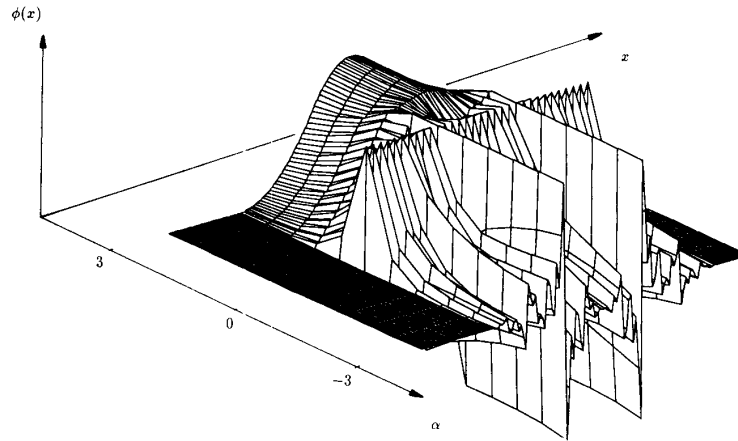


Fig. 14. Scaling function generated by using iteration (28) for  $[1, \alpha, \alpha, 1]$  and  $\alpha \in [-3, 3]$ , (sixth iteration is shown).

#### IV. ALGEBRAIC STRUCTURE OF FIR SOLUTIONS

##### A. Bezout's Identity

From Section III it can be seen using (42), (40), and (43) that the condition to achieve perfect reconstruction with FIR synthesis filters after an FIR analysis section can be expressed in two equivalent forms:

$$H_{00}(z)H_{11}(z) - H_{01}(z)H_{10}(z) = z^{-1} \quad (67)$$

$$H_0(z)H_1(-z) - H_0(-z)H_1(z) = 2z^{-2l-1}. \quad (68)$$

Each of these equations implies the other, and we use (67) or (68) depending on which is more convenient for our purpose. These requirements of course considerably constrain the possible solutions; both (67) and (68) are special forms of what is known as a Bezout identity [43], [44]. This identity arises in the Euclidean algorithm which calculates the greatest common divisor of two polynomials  $a_0(x)$  and  $a_1(x)$ :

$$a_r(x) = \alpha \operatorname{gcd}(a_0(x), a_1(x))$$

where  $a_r(x)$  is the last divisor of the algorithm and  $\alpha$  is a constant. It is well known that we can always write

$$a_r(x) = p_0(x)a_0(x) + p_1(x)a_1(x) \quad \text{for some } p_0(x), p_1(x). \quad (69)$$

If  $a_0(x)$  and  $a_1(x)$  are coprime then  $a_r(x)$  has zeros at 0 or  $\infty$  only; and the identification between (69), the Bezout identity, and (67) or (68) becomes clear. By examining the implications of this, new results emerge; also, from this angle certain results that previously had more involved proofs (e.g., [45]) now become simpler. A review of the necessary properties of the Euclidean algorithm can be found, for example, in [46]. The importance of the algorithm in the context of biorthogonal systems has also been noted in [28] and [47]. The following easily proved fact will play an important role in the rest of this section [46].

*Fact 4.1: Given  $a(x)$  and  $b(x)$*

$$a(x)p(x) + b(x)q(x) = c(x)$$

*has a solution  $[p(x), q(x)] \Leftrightarrow \operatorname{gcd}(a(x), b(x))$  divides  $c(x)$ .*

We now make use of these observations to examine the constraints on the filter banks.

*Proposition 4.2: Assume that the filters  $H_0(z)$  and  $H_1(z)$  are FIR and causal. Then given one of the pairs  $[H_{00}(z), H_{01}(z)]$ ,  $[H_{10}(z), H_{11}(z)]$ ,  $[H_{00}(z), H_{10}(z)]$  or  $[H_{01}(z), H_{11}(z)]$  in order to calculate the other pair necessary to achieve perfect reconstruction it is necessary and sufficient that the given pair be coprime (except for possible zeros at  $z = \infty$ ).*

*Proof:* From fact 4.1 the gcd of each of these pairs must divide the right-hand side of (67). Hence the only factors that they can have in common are zeros at  $z = \infty$ .  $\square$

The above proposition is also proved using a different argument in [45].

*Proposition 4.3: A filter  $H_0(z)$  has a complementary filter if and only if it has no zeros in pairs at  $z = \alpha$  and  $z = -\alpha$ .*

*Proof:*  $H_0(z)$  has a zero pair at  $(\alpha, -\alpha)$  if and only if  $H_0(z)$  has a factor  $A(z^2)$ . This happens if and only if both  $H_{00}(z)$  and  $H_{01}(z)$  have a common factor  $A(z)$ , that is, they are not coprime. Thus the absence of zero pairs of the form  $(\alpha, -\alpha)$  and coprimeness are equivalent and the proof is completed by using proposition 4.2.  $\square$

*Proposition 4.4: There is always a complementary filter to the binominal filter:*

$$H_0(z) = (1 + z^{-1})^k = H_{00}(z^2) + z^{-1}H_{01}(z^2). \quad (70)$$

*Proof:* If  $H_{00}(z)$  and  $H_{01}(z)$  had a common factor it would appear as a pair of zeros of  $H_0(z)$  at  $(\alpha, -\alpha)$ ; since  $H_0(z)$  has zeros only at  $z = -1$  it cannot have such a factor.  $\square$

It should also be clear that for  $H_0(z)$  and  $H_1(z)$  to form a perfect reconstruction pair it is necessary that they be coprime. From fact 4.1 gcd  $[H_0(z), H_1(z)]$  must divide the

right-hand side of (68). This has a very clear signal processing interpretation: a zero common to  $H_0(z)$  and  $H_1(z)$  would imply a transmission null in both channels of the filter bank at some frequency, making reconstruction impossible.

*B. An Analogy with Diophantine Equations*

The conditions under which a complementary filter to some chosen  $H_0(z)$  exist were detailed in Section IV-A. It has already been pointed out that such a filter could be found using Euclid's algorithm; another method of finding a complementary filter based on solving a set of linear equations is given in [21] and Section V-A. The complement is not unique. If given a filter  $H_0(z)$ , we can calculate one of its complements  $H_1(z)$ , it is natural to wonder how we may find others. The results of this section will show that given any complementary filter, a simple mechanism exists for finding all others.

The basic idea again stems from our interpretation of the condition for FIR perfect reconstruction as a Bezout identity. In number theory equations with integer coefficients for which integer solutions are sought are known as diophantine equations [43]. For example,

$$ax + by = c \tag{71}$$

where all quantities are integers and we seek the solution  $(x, y)$  is the most basic diophantine equation. Clearly, if solutions of the equation

$$ax' + by' = 0 \tag{72}$$

are available then we can add them to  $(x, y)$  and generate new solutions to (71). If we replace integers by polynomials then (71) is analogous to the equation for perfect reconstruction that we must solve. We exploit this fact in the rest of this section by noting that polynomial solutions to an equation analogous to (72) are indeed easy to find; this allows us to generate all possible complementary filters if we are first given one. In fact, if we work with the modulation version of the PR condition (68), and identify:  $a = -H_0(z)$  and  $b = H_0(-z)$  it is easy to see that  $[x, y] = [E(z)H_0(-z), E(z)H_0(z)]$  sets the right-hand side to zero if  $E(z) = E(-z)$ .

For the following proposition we make use of proposition A.3, which gives that the length  $N - 2$  linear phase

	$z^0$	$z^{-1}$	$z^{-2}$	$z^{-3}$	$z^{-4}$	$z^{-5}$	$z^{-6}$	$z^{-7}$	$z^{-8}$	$z^{-9}$	$z^{-10}$
$\alpha_1 H_0(z)$	$\alpha_1$	$4\alpha_1$	$6\alpha_1$	$4\alpha_1$	$\alpha_1$						
$z^{-2}\alpha_2 H_0(z)$			$\alpha_2$	$4\alpha_2$	$6\alpha_2$	$4\alpha_2$	$\alpha_2$				
$z^{-4}\alpha_2 H_0(z)$					$\alpha_2$	$4\alpha_2$	$6\alpha_2$	$4\alpha_2$	$\alpha_2$		
$z^{-6}\alpha_1 H_0(z)$							$\alpha_1$	$4\alpha_1$	$6\alpha_1$	$4\alpha_1$	$\alpha_1$
$z^{-4}H_1(z)$					$\frac{1}{16}$	$\frac{1}{4}$	$\frac{1}{16}$				

Giving for  $H'_1(z)$

$$H'_1(z) = [\alpha_1, 4\alpha_1, 6\alpha_1 + \alpha_2, 4\alpha_1 + 4\alpha_2, \frac{1}{16} + \alpha_1 + 7\alpha_2, 8\alpha_2 + \frac{1}{4}, \frac{1}{16} + \alpha_1 + 7\alpha_2, 4\alpha_1 + 4\alpha_2, 6\alpha_1 + \alpha_2, 4\alpha_1, \alpha_1]$$

complementary filter to an odd length  $N$  linear phase filter is unique if it exists.

*Proposition 4.5: Given a linear phase  $H_0(z)$  of odd length  $N$ , and its length  $N - 2$  linear phase complement  $H_1(z)$ , all higher degree odd length linear phase filters complementary to  $H_0(z)$  are of the form*

$$H'_1(z) = z^{-2m}H_1(z) + E(z)H_0(z)$$

where

$$E(z) = \sum_{i=1}^m \alpha_i (z^{-2(i-1)} + z^{-(4m-2i)}).$$

*Proof:* Note that  $E(z) = E(-z)$ , and that  $E(z)H_0(z)$  is symmetric about the point  $(N + 4m - 3)/2$  just as  $z^{-2m}H_1(z)$  is. Hence,  $z^{-2m}H_1(z) + E(z)H_0(z)$  is easily seen to be a linear phase solution of length  $N + 4m - 2$  by direct substitution.

We now show that all length  $N + 4m - 2$  solutions are of this form. If  $H'_1(z)$  is of length  $N + 4m - 2$  then  $H_0(z)H'_1(-z)$  and  $H_0(z)E(z)H_0(-z)$  are both valid and of length  $2N + 4m - 3$ . So also is  $P''(z) = H_0(z)[H'_1(z) - E(z)H_0(-z)]$ . We can choose the coefficients of  $E(z)$  to set some of the end terms of  $P''(z)$  to zero. That is, for some choice of  $\alpha_1$  the coefficients of  $z^0$  and  $z^{-(2N+4m-4)}$  become zero, so that  $P''(z)$  is reduced in length by 4 (the coefficients of  $z^{-1}$  and  $z^{-(2N+4m-5)}$  are already zero). Similarly, for each of the  $\alpha_i$  we can reduce the length of  $P''(z)$  by 4. When  $\alpha_1, \dots, \alpha_m$  have been appropriately fixed  $P''(z)$  has length  $2N - 3$ , has powers of  $z^{-1}$  in the range  $z^{-2m}$  to  $z^{-2m+2N-4}$  and is still valid. Since it contains  $H_0(z)$  as a factor it must have the form

$$P''(z) = z^{-2m}H_0(z)H_1(-z)$$

since the length  $N - 2$  solution is unique by proposition A.3.  $\square$

From proposition 3.3 it follows that in the two nontrivial cases of linear phase solutions, the length of  $P(z) = H_0(z)H_1(-z)$  is  $4n - 1$ . In Appendix A.4 it is shown that the solutions indicated in proposition 3.3 b) are special cases of those in a); that is, they can always be refactored into the form a). It follows that all higher degree complementary filters to a fixed  $H_0(z)$  are given by proposition 4.5, unless they are trivial, in the sense of belonging to class c) of proposition 3.3.

*Example:* Consider  $H_0(z) = [1, 4, 6, 4, 1]$  and its unique length 3 complementary filter  $H_1(z) = [1, 4, 1]/16$ . Let  $m = 2$ . So we get

which is linear phase, and complementary to  $H_0(z)$ .

A further result allows us to use the diophantine equa-

tions to reach more general solutions. For this we use the result (from proposition A.2) that a length  $N$  filter has  $N - 2$  length  $N - 2$  complementary filters.

*Proposition 4.6:* All filters of length  $N + 2m - 2$  which are complementary to a length  $N$  filter  $H_0(z)$  have the form

$$H_1'(z) = z^{-2k}H_1(z) + E(z)H_0(z)$$

where  $E(z) = E(-z)$  is a polynomial of degree  $2(m - 1)$ ,  $k \in \{0, 1, \dots, m\}$  and  $H_1(z)$  is a length  $N - 2$  complementary filter.

*Proof:* That this is a solution is easily verified by substitution. If

$$E(z) = \sum_{i=0}^{m-1} \beta_i z^{-2i}$$

then  $P''(z) = H_0(z)[H_1'(-z) - E(z)H_0(-z)]$  is reduced in length by 2 for some choice of  $\beta_0$  or  $\beta_{m-1}$ . Again the argument is repeated; the length of  $P''(z)$  can be reduced by 2 at each stage by fixing one of the  $\beta_i$ . In this way we reduce the degree of  $P''(z)$  by  $2m$  when all of the  $\beta_i$ 's are appropriately chosen. Since  $H_0(z)$  is still a factor, the remaining factor must be one of the length  $N - 2$  solutions of which there are only  $N - 2$ .  $\square$

So far we have addressed only the problem of generating higher degree solutions from lower ones; the next proposition shows that we can also go in the opposite direction. We examine the linear phase case only; the extension to the general case is obvious. For the linear phase case this says that given any complementary filter we can generate all others using the results of proposition 4.5.

*Proposition 4.7:* If  $H_1^{(2)}(z)$  and  $H_1^{(1)}(z)$  are length  $N + 4m_2 - 2$ , and length  $N + 4m_1 - 2$  linear phase complementary filters to the linear phase odd length  $N$  filter  $H_0(z)$ , with  $m_2 > m_1$  then we can generate the lower degree solution from the higher as follows:

$$H^{(1)}(z) = z^{2(m_2 - m_1)} [H_1^{(2)}(z) + E_3(z)H_0(z)]$$

where  $E_3(z) = z^{-2(m_2 - m_1)}E_1(z) - E_2(z)$ .

*Proof:* Direct substitution.  $\square$

The subclass of all valid  $P(z)$ 's which can be factored as  $P(z) = H_0(z)H_0(z^{-1})$  corresponds to paraunitary FB's, and generates orthonormal bases of wavelets. Since all such  $P(z)$ 's are symmetric and positive they form a subclass of those generated by the construction of proposition 4.5 above. The case for which  $H_0(z)$  is chosen to be an even power of the binomial is treated in detail by Daubechies. In Appendix A.5 we establish the close relation between her results and proposition 4.5 above. The fact that higher degree solutions contain lower degree ones is also given in [47].

### C. Continued Fraction Expansions

In Section IV-B it was shown that any solution to (67) or (68) could be written as the sum of lower degree solutions and trivial higher degree solutions (trivial in the sense that the right hand side of (44) becomes zero). In Section IV-B we dealt exclusively with the modulation

domain; but the results there, like those of this section could be expressed in either modulation or polyphase notation. For the sake of definiteness consider the polyphase version of the perfect reconstruction condition (67), and assume that  $H_{00}(z)$  and  $H_{01}(z)$  are given. It can be seen from proposition 4.6 that this lowest degree solution is in some sense fixed, and embedded at the core of any higher degree solution. The strong connections between Euclid's algorithm, the Bezout identity and continued fraction expansions (CFE's) is well known [43], [48]. In fact, we now show that the canonic CFE of  $H_{10}/H_{11}$  is the same as that of  $H_{00}/H_{01}$  except for the last term; and further that higher degree solutions are formed by adding terms to the CFE, the first terms remaining unchanged.

We define  $D_{-1} = H_{00}$ ,  $D_0 = H_{01}$ ,  $A_{-1} = H_{10}$ , and  $A_0 = H_{11}$ . For the sake of simplicity we remove the phase factor in (67). In this notation (67) becomes

$$D_{-1}(z)A_0(z) - A_{-1}(z)D_0(z) = 1. \quad (73)$$

Now use Euclid's algorithm starting with the pair  $D_{-1}(z)$ ,  $D_0(z)$ . The first step gives

$$D_{-1}(z) = b_0(z)D_0(z) + D_1(z) \quad \deg D_0 > \deg D_1.$$

Also do one division of the pair  $A_{-1}(z)$ ,  $A_0(z)$ , denoting the remainder  $A_1(z)$ :

$$A_{-1}(z) = a_0(z)A_0(z) + A_1(z) \quad \deg A_0 > \deg A_1.$$

Together these equations give

$$\begin{aligned} 1 &= D_{-1}(z)A_0(z) - A_{-1}(z)D_0(z) \\ &= (b_0(z) - a_0(z))A_0(z)D_0(z) + D_1(z)A_0(z) - A_1(z)D_0(z). \end{aligned}$$

However, since  $\deg A_0 D_0 > \deg D_1 A_0$  and  $\deg A_0 D_0 > \deg D_0 A_1$  must have  $a_0 = b_0$ , and hence

$$D_0(z)A_1(z) - A_0(z)D_1(z) = -1.$$

Since this is of the same form, but of lower degree, than the equation that we started with (73), we can compare the second step of Euclid's algorithm with a division of  $A_0(z)$ ,  $A_1(z)$  and this gives  $a_1(z) = b_1(z)$ . The result is that we get a succession of Bezout identities:

$$D_{j-1}(z)A_j(z) - D_j(z)A_{j-1}(z) = (-1)^j \quad (74)$$

which are of decreasing degree. We find in turn that  $a_0(z) = b_0(z)$ ,  $a_1(z) = b_1(z)$ ,  $\dots$ ,  $a_j(z) = b_j(z)$ ,  $\dots$ ,  $a_N(z) = b_N(z)$ . Note that these outputs of Euclid's algorithm are the partial denominators of the canonical CFE of  $D_{-1}(z)/D_0(z)$  [48], [43]:

$$\begin{aligned} \frac{D_{-1}(z)}{D_0(z)} &= \frac{H_{00}(z)}{H_{01}(z)} = b_0(z) + \frac{1}{b_1(z) + \frac{1}{b_2(z) + \frac{1}{\dots + \frac{1}{b_N(z)}}}} \\ &= [b_0(z); b_1(z), b_2(z), \dots, b_N(z)] \end{aligned}$$

where we have used the standard notation  $[b_0; b_1, b_2, \dots$

$b_N$ ] to denote a terminating CFE [49]. It follows that the CFE's of  $D_{-1}(z)/D_0(z)$  and  $A_{-1}(z)/A_0(z)$  are identical for the first  $N + 1$  terms. The terminal equation for  $j = N$  gives

$$A_{N-1}(z) = \frac{D_{N-1}(z)A_N(z) - (-1)^N}{D_N}. \quad (75)$$

Remark that the  $D_j(z)$ 's are known, and  $D_N$  is a scalar (since it is the last divisor and  $D_{-1}(z), D_0(z)$  are assumed to be coprime); hence we can choose  $A_N(z)$  to be any polynomial and we are assured that  $A_j(z)$ 's are polynomial for  $j = N - 1, \dots, 0, -1$ . Therefore we get a valid complementary filter  $[A_0(z), A_{-1}(z)]$  for any appropriate  $A_N(z)$ . This can be expressed by writing  $a_{N+1}(z) = (-1)^N A_N(z) D_N$ . In summary,

$$\frac{H_{00}(z)}{H_{01}(z)} = [b_0(z); b_1(z), b_2(z), \dots, b_N(z)] \quad (76)$$

$$\frac{H_{10}(z)}{H_{11}(z)} = [b_0(z); b_1(z), b_2(z), \dots, b_N(z), -(-1)^N A_N(z) D_N]. \quad (77)$$

It can be shown that choosing  $A_N(z) = 0$  gives the same solution as that produced by Euclid's algorithm. That is,

$$\frac{H_{10}(z)}{H_{11}(z)} = [b_0(z); b_1(z), \dots, b_{N-1}(z), b_N(z), 0] \\ = [b_0(z); b_1(z), \dots, b_{N-1}(z)].$$

If we divide (74) by  $D_j(z)D_{j-1}(z)$  we get

$$\frac{A_j(z)}{D_j(z)} - \frac{A_{j-1}(z)}{D_{j-1}(z)} = \frac{(-1)^j}{D_j(z)D_{j-1}(z)} \quad (78)$$

which is the expression relating successive convergents to a CFE [50]. This is precisely the continued fraction in (76), (77). Note that since the successive convergents satisfy the decreasing degree Bezout identities (74), truncating (76) and (77) gives a lower degree FIR PRFB.

There is more structure yet. Dividing (74) by  $D_{j-1}(z)A_{j-1}(z)$  gives

$$\frac{A_j(z)}{A_{j-1}(z)} - \frac{D_j(z)}{D_{j-1}(z)} = \frac{(-1)^j}{A_{j-1}(z)D_{j-1}(z)}.$$

Like (78) this relates successive convergents of a continued fraction; but the CFE here is that of a different grouping of the polyphase pairs. It turns out that we get

$$\frac{H_{10}(z)}{H_{00}(z)} = [(-1)^N A_N(z) D_N; b_N(z), b_{N-1}(z), \dots, b_0(z)]$$

$$\frac{H_{11}(z)}{H_{01}(z)} = [(-1)^N A_N(z) D_N; b_N(z), b_{N-1}(z), \dots, b_1(z)].$$

Of course, these continued fraction relations give another method for generating higher degree solutions to the perfect reconstruction condition. By varying  $A_N(z)$  in (77) for example we generate different complementary filters.

Clearly, this structure is complete; all possible complementary filters can be generated by appropriate choice of  $A_N(z)$ .

It warrants reiteration that the above analysis using the polyphase notation, can be used to give equivalent results in the modulation notation.

## V. DESIGN RESULTS

### A. Linear Phase Filters with a Maximum Number of Zeros at $\pi$

We now design a linear phase  $P(z) = H_0(z)H_1(-z)$  satisfying (68) and having the maximum possible number of zeros at  $z = -1$ . Note that if  $P(z)$  has even a single zero at  $z = -1$  it cannot have any at  $z = 1$  and vice versa. This should be clear since we wish to have  $P(z) - P(-z)$  equal to  $2z^{-2l-1}$  (see Section III-A). We consider only the case where  $P(z)$  is of odd length (see proposition 3.3); hence it has an even number of zeros; since  $P(z)$  is linear phase its zeros must occur in quads, and pairs on the unit circle or real axis. It follows that  $P(z)$  must have an even number of zeros at  $z = -1$  or none at all.

Note that by proposition 4.4 we are assured that there exists a complementary filter to the binomial of any degree. We wish now to calculate  $R_{2k}(-z)$  which is the complementary filter to  $(1 + z^{-1})^{2k}$ . In other words, we wish to find the polynomial such that  $P(z) = (1 + z^{-1})^{2k} R_{2k}(z)$  is valid, as defined by (44). That  $R_{2k}(z)$  is linear phase is an immediate consequence of the fact that  $P(z)$  and  $(1 + z^{-1})^{2k}$  are. Because of this symmetry, on equating the appropriate terms to zero it turns out that only  $k$  of the equations are independent; so we get a set of  $k$  by  $k$  equations to be solved for the coefficients  $(r_0, r_1, \dots, r_{k-1})$  [24].

*Example:* If we choose  $F_0(z) = (1 + z^{-1})^6$  we solve the 3 by 3 system found by imposing the constraints on the coefficients of the odd powers of  $z^{-1}$  of

$$P(z) = (r_0 + r_1 z^{-1} + r_2 z^{-2} + r_1 z^{-3} + r_0 z^{-4}) \\ \cdot (1 + 6z^{-1} + 15z^{-2} + 20z^{-3} + 15z^{-4} \\ + 6z^{-5} + z^{-6}).$$

So we solve

$$\begin{pmatrix} 6 & 1 & 0 \\ 20 & 16 & 6 \\ 12 & 30 & 20 \end{pmatrix} \begin{pmatrix} r_0 \\ r_1 \\ r_2 \end{pmatrix} = \begin{pmatrix} 0 \\ 0 \\ 1 \end{pmatrix}$$

giving  $r_6 = (3/2, -9, 19)/128$ .

In general therefore we solve the system

$$F_{2k} \cdot r_{2k} = e_{2k} \quad (79)$$

where  $F_{2k}$  is the  $k \times k$  matrix,  $r_{2k} = (r_0, \dots, r_{k-1})$  and  $e_{2k}$  is the length  $k$  vector  $(0, 0, \dots, 1)$ .

Having found the coefficients of  $R_{2k}(z)$  we factor it into

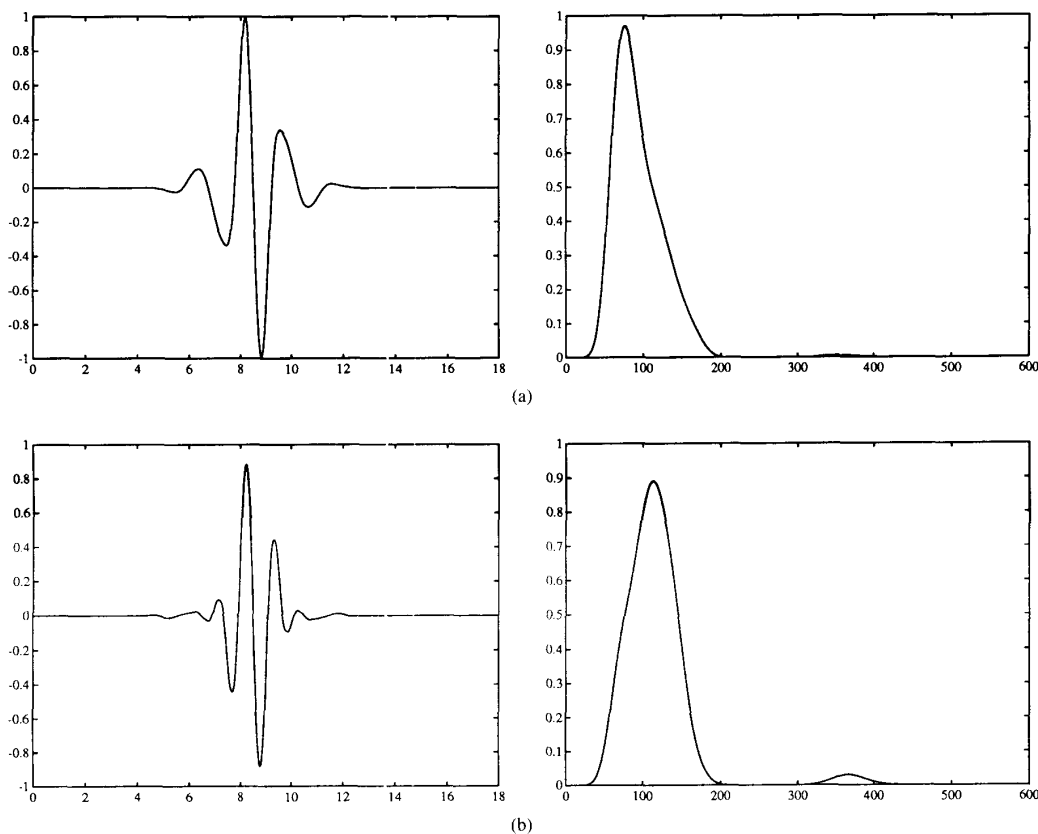


Fig. 15. Biorthogonal wavelets generated by the length 18 filters given in Tables I and II. The filters have a maximum number of zeros at  $z = -1$ . (a) Time function and spectrum of analysis wavelet. (b) Time function and spectrum of synthesis wavelet.

TABLE I  
IMPULSE RESPONSE COEFFICIENTS OF  
BIORTHOGONAL  $H_0(z)$ ; THE INFINITE  
ITERATION OF THESE FILTERS GIVE  
THE WAVELETS SHOWN IN FIG. 15

$H_0(z)$		
$h_0(0)$	0.00122430	$h_0(17)$
$h_0(1)$	-0.00069860	$h_0(16)$
$h_0(2)$	-0.01183749	$h_0(15)$
$h_0(3)$	0.01168591	$h_0(14)$
$h_0(4)$	0.07130977	$h_0(13)$
$h_0(5)$	-0.03099791	$h_0(12)$
$h_0(6)$	-0.22632564	$h_0(11)$
$h_0(7)$	0.06927336	$h_0(10)$
$h_0(8)$	0.73184426	$h_0(9)$

TABLE II  
IMPULSE RESPONSE COEFFICIENTS OF  
BIORTHOGONAL  $H_1(z)$ ; THE INFINITE  
ITERATION OF THESE FILTERS GIVE  
THE WAVELETS SHOWN IN FIG. 15

$H_1(z)$		
$h_1(0)$	0.00122430	$-h_1(17)$
$h_1(1)$	0.00069979	$-h_1(16)$
$h_1(2)$	-0.01134887	$-h_1(15)$
$h_1(3)$	-0.01141245	$-h_1(14)$
$h_1(4)$	0.02347331	$-h_1(13)$
$h_1(5)$	0.00174835	$-h_1(12)$
$h_1(6)$	-0.04441890	$-h_1(11)$
$h_1(7)$	0.20436993	$-h_1(10)$
$h_1(8)$	0.64790805	$-h_1(9)$

linear phase components; and then regroup these factors of  $R_{2k}(z)$ , and the  $2k$  zeros at  $z = -1$  to form two filters:  $H_0(z)$  and  $H_1(-z)$ , both of which are to be regular.

It turns out that for small  $k$ , ensuring that both  $H_0(z)$  and  $H_1(-z)$  meet the bound of proposition 2.1 can force one to choose filters of quite unequal length. For larger  $k$ , however, this problem eases, and it becomes possible to get filters of the same, or approximately the same, length that generate regular symmetric wavelets. For example,

Fig. 15 shows the analysis and synthesis wavelets and their spectra for one particular factorization of the  $k = 9$  case, and Tables I and II list the coefficients of the filters  $H_0(z)$  and  $H_1(-z)$ . Each of these filters has a factor  $(1 + z^{-1})^9$ . We get  $H_0(z) = [(1 + z^{-1})/2]^9 F_0(z)$  where  $\sup_{\omega \in [0, 2\pi]} |F_0(e^{j\omega})| \approx 115.06 < 2^8$ , so  $H_0(z)$  satisfies the bound of proposition 2.1. Hence the scaling function  $\phi(x)$  and wavelet  $\psi(x)$  generated by the infinite iterations, following (59) and (61), converge to continuous functions.

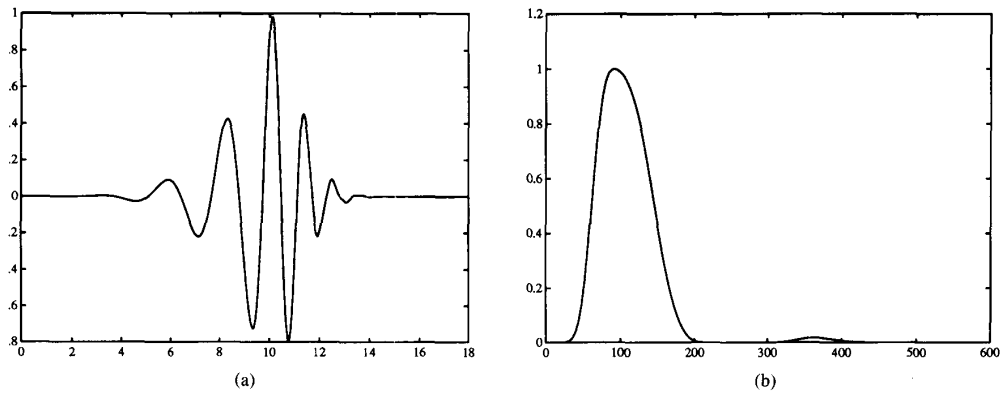


Fig. 16. Orthonormal wavelet generated by length 18 filter (from [12]). The filter has a maximum number of zeros at  $z = -1$ . (a) Time function. (b) Spectrum.

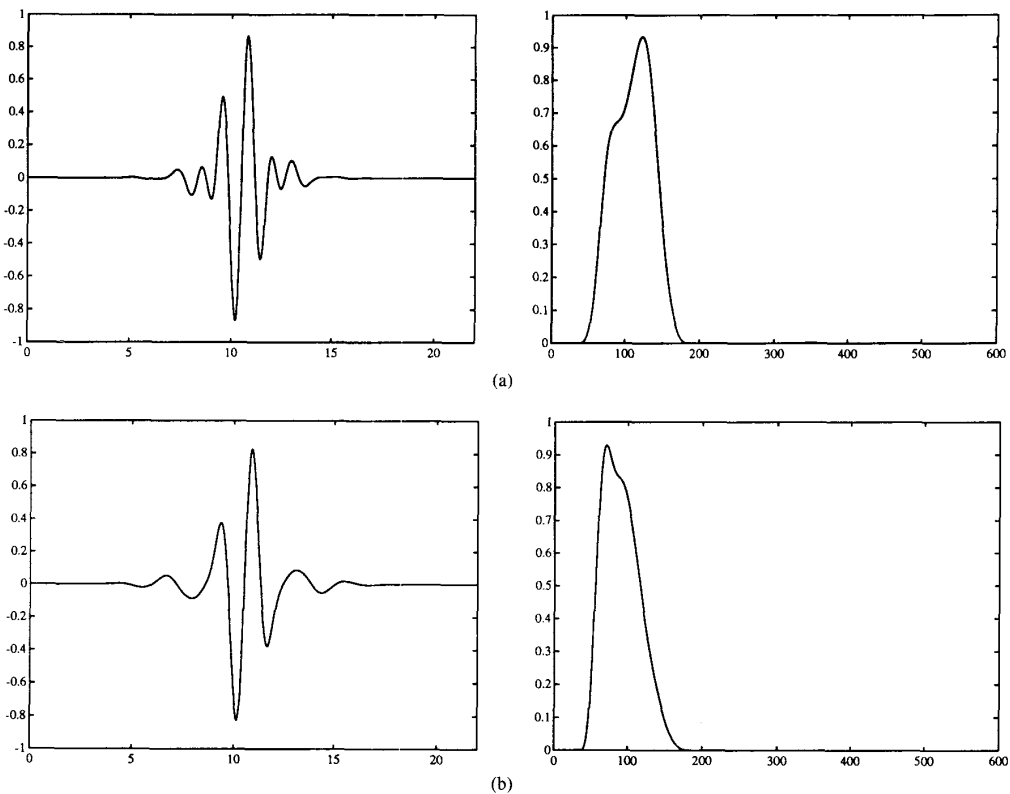


Fig. 17. Biorthogonal wavelets generated by filters of length 20 and 24 given in Tables III and IV. The filters were designed using the diophantine approach, and have better stopband performance than those in Fig. 15. (a) Time function and spectrum of analysis wavelet. (b) Time function and spectrum of synthesis wavelet.

$H_1(-z)$  can be similarly factored, and  $\sup_{\omega \in [0, 2\pi]} |F_1(e^{j\omega + \pi})| \approx 211.3 < 2^8$ ; hence  $\check{\phi}(x)$  and  $\check{\psi}(x)$  converge to continuous functions also.

The method outlined in [35] yields the following estimates for the regularity index  $\beta$ : for  $\psi(x)$  we find  $2.46 < \beta$ , and for  $\check{\psi}(x)$  we get  $3.55 < \check{\beta}$ .

For comparison purposes we show in Fig. 16 the corresponding plots for the orthonormal wavelet generated by a filter of the same length, as presented in [12].

**B. More General Solutions: Diophantine Approach**

While the design procedure of the previous section is very simple, the spectra of the scaling function  $\Psi(\omega)$  and the wavelet  $\Phi(\omega)$  are not as one might wish from low-pass and bandpass filters.

Proposition 4.5 showed how to generate any valid linear phase  $P(z)$  containing a given factor. For example, to design a  $P(z)$  with  $2k$  zeros at  $\pi$ , we can calculate  $R_{2k}(-z)$ ,

TABLE III  
IMPULSE RESPONSE COEFFICIENTS OF IMPROVED  
BIORTHOGONAL  $H_0(z)$ ; THE INFINITE ITERATION  
OF THESE FILTERS GIVE THE WAVELETS  
SHOWN IN FIG. 17

$H_0(z)$		
$h_0(0)$	0.00133565	$h_0(23)$
$h_0(1)$	-0.00201229	$h_0(22)$
$h_0(2)$	-0.00577577	$h_0(21)$
$h_0(3)$	0.00863853	$h_0(20)$
$h_0(4)$	0.01279957	$h_0(19)$
$h_0(5)$	-0.02361445	$h_0(18)$
$h_0(6)$	-0.01900852	$h_0(17)$
$h_0(7)$	0.04320273	$h_0(16)$
$h_0(8)$	-0.00931630	$h_0(15)$
$h_0(9)$	-0.12180846	$h_0(14)$
$h_0(10)$	0.05322182	$h_0(13)$
$h_0(11)$	0.41589714	$h_0(12)$

as in the previous section. This solution, which has degree  $2k - 2$ , can then be used to generate all possible solutions of degree  $2k - 2 + 2m$ .

A second approach is to note that we need not place all of the zeros at  $z = -1$  to start with. We could for example calculate the complementary filter to a factor  $(1 + z^{-1})^{2j} [u_1(z)u_2(z) \cdots u_l(z)]^2$  where  $u_i(z)$  represents a zero pair on the unit circle. We are then assured of having a factor  $(1 + z^{-1})^j [u_1(z)u_2(z) \cdots u_l(z)]$  to place in the stopband of each of the filters.

In Fig. 17 we show the two symmetric wavelets  $\psi(t)$  and  $\check{\psi}(t)$  and their spectra. These were generated by linear phase filters of lengths 24 and 20, the coefficients of which are listed in Tables III and IV. The filters were designed using a combination of the two approaches described above. Each of the filters has only a single zero at  $z = -1$ , and neither of them meets the bound given in proposition 2.1. However again using the estimation methods of [35] we find  $0.79 < \beta$  and  $0.96 < \check{\beta}$ . Note that the stopband performance is much better than in Figs. 15 and 16.

Fig. 18 shows the wavelet and its spectrum for a better orthogonal set of filters. The associated filter bank is paraunitary; so  $H_1(z) = H_0(z^{-1})$ . The coefficients are listed in Table V. The regularity estimate here is  $0.97 < \beta$ .

### C. Root Loci of Higher Degree Solutions

While we have shown that higher degree solutions can give better results, it is still clear from Sections IV-B and IV-C that these solutions are nonetheless very constrained. To give a concrete example we briefly examine the case where  $H_0(z) = (1 + z^{-1})^6$  and the unique linear phase degree 4 complementary filter has impulse response coefficients  $h_1(n) = [3, 18, 38, 18, 3]/256$ . We examine the  $m = 1$  solution (from proposition 4.5)

$$H'_1(z) = z^{-2}H_1(z) + \alpha(1 + z^{-2})H_0(z) \quad (80)$$

TABLE IV  
IMPULSE RESPONSE COEFFICIENTS OF IMPROVED  
BIORTHOGONAL  $H_1(z)$ ; THE INFINITE ITERATION  
OF THESE FILTERS GIVE THE WAVELETS  
SHOWN IN FIG. 17

$H_1(z)$		
$h_1(0)$	0.00465997	$-h_1(19)$
$h_1(1)$	0.00702071	$-h_1(18)$
$h_1(2)$	-0.01559987	$-h_1(17)$
$h_1(3)$	-0.02327921	$-h_1(16)$
$h_1(4)$	0.05635238	$-h_1(15)$
$h_1(5)$	0.10021543	$-h_1(14)$
$h_1(6)$	-0.06596151	$-h_1(13)$
$h_1(7)$	-0.13387993	$-h_1(12)$
$h_1(8)$	0.38067810	$-h_1(11)$
$h_1(9)$	1.10398118	$-h_1(10)$

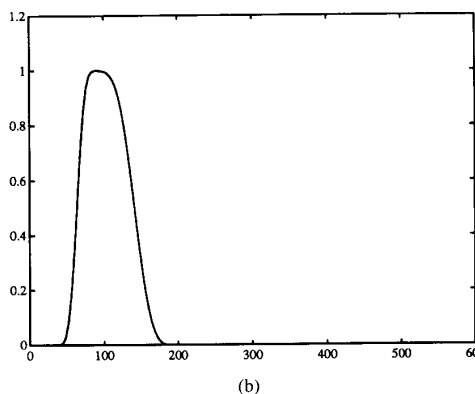
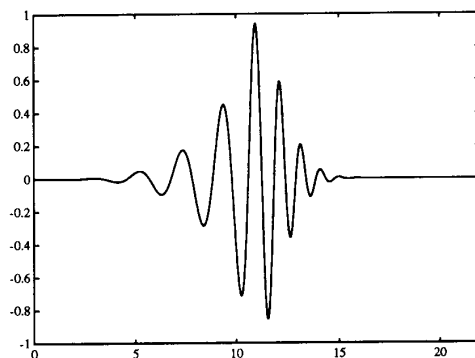


Fig. 18. Orthonormal wavelet generated by length 22 filter given in Table V. The filter was designed using the diophantine approach, and has better stopband performance than that in Fig. 16. (a) Time function. (b) Spectrum.

and plot the trajectory in the  $z$  plane of the roots as  $\alpha$  is varied.

Fig. 19 shows the root locus for the region:  $\alpha \in [-2, 2]$ . While the increased degree solution has more freedom, it is clear that the roots move along very constrained paths. In other words, it would be necessary to look at solutions of considerably higher degree to get substantial design freedom.

TABLE V  
IMPULSE RESPONSE OF IMPROVED  
PARAUNITARY FACTORIZATION:  
THE INFINITE ITERATION GIVES  
THE WAVELET SHOWN IN  
FIG. 18

	$H_0(z)$
$h_0(0)$	0.055739
$h_0(1)$	0.288322
$h_0(2)$	0.614682
$h_0(3)$	0.608634
$h_0(4)$	0.113646
$h_0(5)$	-0.290892
$h_0(6)$	-0.131805
$h_0(7)$	0.162510
$h_0(8)$	0.085330
$h_0(9)$	-0.099666
$h_0(10)$	-0.042965
$h_0(11)$	0.060044
$h_0(12)$	0.015233
$h_0(13)$	-0.032323
$h_0(14)$	-0.001634
$h_0(15)$	0.014199
$h_0(16)$	-0.002305
$h_0(17)$	-0.004433
$h_0(18)$	0.001808
$h_0(19)$	0.000646
$h_0(20)$	-0.000577
$h_0(21)$	0.000111

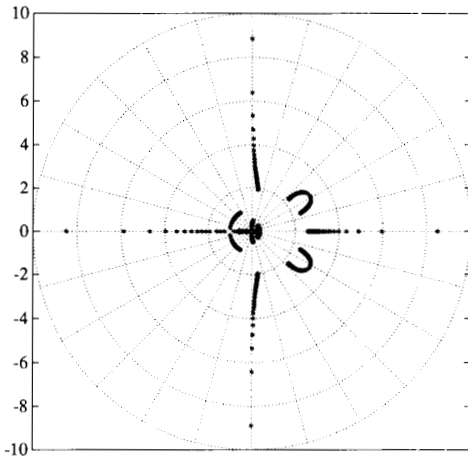


Fig. 19. Locus of the movement of the roots of (80) in the  $z$  plane for  $\alpha \in [-2, 2]$ .

VI. CONCLUSION

The relationships between wavelets, multiresolution signal analysis, and filter banks have been developed, emphasizing the equivalence between the fundamental ideas of each of these fields, which is that functions or signals be broken down into component signals at different resolutions. In addition, strong similarities between the details of these techniques have been pointed out, and the interplay of ideas has enabled us to indicate new results in each of the areas.

In particular, we derived biorthogonal compactly supported wavelets bases with symmetries using regular FIR

PRFB's. If compact support is not desired, similar techniques, using IIR filters generate orthogonal wavelet bases with symmetries [25], [51].

APPENDIX A

1. Biorthogonal Pyramid

This Appendix extends the result of Section II-D to the biorthogonal case (see also Section III-C). In this case, the approximation  $\bar{x}$  is equal to

$$\bar{x} = G_0 H_0 \cdot x.$$

The difference signal becomes

$$d = (I - G_0 H_0)x = G_1 H_1 \cdot x.$$

Because we have perfect reconstruction:

$$G_0 H_0 + G_1 H_1 = I.$$

That is, we can filter the difference signal with  $h_1(n)$  and subsample by 2, because

$$H_1 G_1 H_1 = H_1$$

from which  $d$  can be reconstructed by upsampling and interpolation with  $G_1$ , following the fact that

$$G_1 H_1 G_1 H_1 = G_1 H_1$$

and the reconstructed signal, obtained by adding  $\bar{x}$  to  $d$ , is equal to the original. That is, the biorthonormal pyramid is equivalent to a critically sampled biorthogonal filter bank. Note that linear processing has been assumed throughout, which would not be the case in coding applications.

2. Proof of Proposition 3.3

*Proof:* Since  $H_0(z)$  and  $H_1(-z)$  have linear phase so does  $P(z)$ . If  $P(z)$  has odd length, then both filters have odd length or both have even length. Note that

$$\begin{aligned} P(z) - P(-z) &= \sum_{i=0}^{2N} p_i z^{-i} [1 - (-1)^i] \\ &= \sum_{i=0}^{N-1} 2p_{2i+1} z^{-(2i+1)}. \end{aligned}$$

Since  $P(z)$  is of odd length, both  $P(z)$  and  $P(-z)$  are symmetric or antisymmetric about the point  $i = N$ . Hence,  $P(z) - P(-z)$  is symmetric about this point; so the single nonzero coefficient is  $p_N$ , the central one. Hence  $P(z)$  is symmetric and not antisymmetric; which implies that  $H_0(z)$  and  $H_1(-z)$  are both symmetric or antisymmetric.

a)  $L_0$  and  $L_1$  both odd. Now  $L_0 + L_1 - 1$  is odd. The center of symmetry, which is  $(L_0 + L_1)/2 - 1$  samples away from the end points, has to be odd. Thus  $(L_0 + L_1)/2 = L_0 + (L_0 - L_1)/2$  has to be even. Thus  $(L_0 - L_1)/2$  is odd, and the length difference  $L_0 - L_1$  is an odd multiple of 2. In particular, there are no same length solutions. Suppose that  $H_0(z)$  and  $H_1(-z)$  can be both symmetric or both antisymmetric. The latter possibility is ruled out, however, because the two polyphase compo-

nents are also antisymmetric when the length is odd, and are therefore not coprime. Perfect reconstruction is then impossible following proposition 4.2.

b)  $L_0$  and  $L_1$  both even. Again  $(L_0 + L_1)/2 - 1$  has to be odd so that the center term is not in the same set as the end terms. Then  $L_0 + (L_0 - L_1)/2$  has to be even, and since  $L_0$  is even, this means that the length difference  $L_0 - L_1$  is an even multiple of 2; and, for example, same length solutions do exist. Also it was assumed that  $H_0(z)$  and  $H_1(-z)$  were both symmetric, but since  $H_1(-z)$  has opposite symmetry to  $H_1(z)$  when the length is even, the even length solution leads to a symmetric/antisymmetric pair.

c) If  $P(z)$  has even length, then one filter has even length, and one odd. Now we get

$$\begin{aligned} P(z) - P(-z) &= \sum_{i=0}^{2N-1} p_i z^{-i} [1 - (-1)^i] \\ &= \sum_{i=0}^{N-1} 2p_{2i+1} z^{-(2i+1)}. \end{aligned}$$

$P(z)$  has only a single nonzero odd-indexed coefficient; but note that  $p_i = \pm p_{2N-1-i}$   $i = 0, \dots, N-1$ . So odd-indexed coefficients are paired with even-indexed-ones. It follows that  $P(z)$  also has only one nonzero even-indexed coefficient, and is of the form

$$P(z) = p_j z^{-j} (1 \pm z^{2N-1-2j}). \quad (81)$$

Since  $P(z)$  has all its zeros on the unit circle (at the  $2(N-j) - 1$  roots of  $\pm 1$ ),  $H_0(z)$  and  $H_1(-z)$  also have all zeros on unit circle. If  $H_0(z)$  and  $H_1(z)$  are both to be antisymmetric, both must have zeros at  $z = 1$ . This will force  $H_1(-z)$  to have a zero at  $z = 1$  or  $z = -1$  depending on whether it is of odd or even length, respectively. This implies that  $P(z)$  has either a double zero at  $z = 1$ , or a pair at  $z = 1$  and  $z = -1$ . Since  $P(z)$  contains only the  $2(N-j) - 1$  roots of  $\pm 1$  both possibilities are ruled out. Hence the filters must have opposite symmetry.  $\square$

### 3. Lattice Structures Generating the Binomial Filter and its Complementary Filter

*Proposition A.1:* Let the polyphase components of  $H_0(z)$  and  $H_1(z)$  be generated by the following lattice structure:

$$H_p(z) = \begin{bmatrix} 1 & 1 \\ 1 & -1 \end{bmatrix} \prod_{i=1}^N \begin{bmatrix} 1 & 0 \\ 0 & z^{-1} \end{bmatrix} \begin{bmatrix} 1 & \alpha_i \\ \alpha_i & 1 \end{bmatrix} \quad (82)$$

then the choice

$$\begin{aligned} (\alpha_1, \alpha_2, \dots, \alpha_N) \\ = ((2N+1)/(2N-1), (2N-1)/(2N-3), \dots, \\ 2N+1) \end{aligned}$$

leads to

$$H_0(z) = (1 + z^{-1})^{2N+1}.$$

An elegant proof of this proposition was pointed out to us

by Gopinath [52]. It is clear that the complementary filter has only rational coefficients.

Now  $P(z)$  can be written as

$$P(z) = H_0(z)H_1(-z) = (1 + z^{-1})^{2k} R_{2k}(z).$$

Since  $R_{2k}(re^{j\theta})$  is linear phase it can be converted into a polynomial of degree  $k-1$  in  $\cos(\theta - j \ln r)$ . Thus the size of the factorization to be performed is halved, and the accuracy of the solution is improved. If the exact rational coefficients of  $R_{2k}(z)$  are used and this is factored in  $\cos z$ , the solution can be considerably more accurate than if a standard linear equation solver is used and direct factorization is performed. We will consider  $k=6$  to give an example of the importance of these considerations. Denote  $P_6(z)$  which is exact,  $P'_6(z)$  which is found by multiplying out after using the lattice outputs given by proposition A.1 and the efficient factorization;  $P''_6(z)$  is found by multiplying out after using an ordinary linear equation solver, and direct factorization. We find  $\|p_6(n) - p'_6(n)\|_\infty = 0.00892$  while  $\|p_6(n) - p''_6(n)\|_\infty = 17.83739$ .

### 4. Restrictions on Complementary Filter Forms

*Proposition A.2:* A length  $N$  filter has at most  $N-2$  complementary filters of length  $N-2$ ; and at most one of length  $N-1$ .

*Proof:* If  $H_1(z)$  has length  $N-2$  then  $P(z) = H_0(z)H_1(-z)$  has length  $2N-3$ ; hence it has  $N-2$  odd-indexed coefficients. Thus we solve a square system of linear equations of size  $N-2$ . The nonzero odd-indexed coefficient can be placed in any of  $N-2$  positions.

If  $H_1(z)$  has length  $N-2$  then  $P(z) = H_0(z)H_1(-z)$  has length  $2N-2$ ; one of the end terms is odd indexed while the other is even. There are  $N-1$  odd-indexed terms. Thus we solve a size  $N-1$  square system, but there is only one possible position for the single nonzero odd-indexed term, which must appear at an end.  $\square$

*Proposition A.3:* For the linear phase case, if a filter of even length  $N$  has a same length complementary filter it is unique. For  $N$  odd if there is a length  $N-2$  complementary filter it is unique.

*Proof:*  $N$  even gives  $N/2$  equations in  $N/2$  unknowns; the nonzero coefficient must be in the center. Similarly,  $N$  odd gives  $(N-1)/2$  equations in  $(N-1)/2$  unknowns.  $\square$

*Note:* An example of the equations to be solved in the linear phase case is given in Section V-A. In propositions A.2 and A.3 it is of course possible that the linear systems to be solved are singular, in which case the complementary filter does not exist (see Section IV-A for necessary and sufficient conditions). It is also possible that on solving the linear system one or more of the end terms of the complementary filter found are zero, in which case it fails to have the advertised length. For example, if we try to find the linear phase length 5 complement to the length 7 filter  $H_0(z) = [1, 0, 0, -1, 0, 0, 1]$  we find  $H_1(z) = [0, 0, 1, 0, 0]$ . For the purposes of propositions 4.5 and 4.6 this case, where the complementary filter has less than the

expected length, has no effect provided that the zero end terms are included.

Of the three classes of linear phase FIR solutions given in proposition 3.3, we note that solutions of class b) can always be refactored to ones of class a). Suppose in a class b) solution  $H_1(z)$  is the antisymmetric filter; it then necessarily has a zero  $1 - z^{-1}$ , which implies that  $H_1(-z)$  has a zero  $1 + z^{-1}$ . This zero can be given to  $H_0(z)$ . Both filters are now of odd length, and differ by an odd multiple of 2. Hence, we have a class a) solution. The converse is not in general true.

### 5. Relation to Work of Daubechies

We here establish the connection between proposition 4.5 and a result given in a different form in [12].

Daubechies writes:  $P^{(1)}(z) = (1 + z^{-1})^{2k} Q^{(1)}(z)$ ; except for a phase factor this gives

$$P(w) = \left( \frac{e^{-jw/2} + e^{jw/2}}{2} \right)^{2k} Q(w).$$

Since  $Q(w)$  is symmetric it can be written as a polynomial in  $\cos(w) = 1/2(1 - \cos^2(w/2))$  when restricted to the unit circle. So if we define  $y = \cos^2(w/2)$  and we can rewrite the above as

$$P(w) = [\cos^2(w/2)]^k Q_{1/2}(1 - \cos^2(w/2))$$

$$P(y) = y^k Q_{1/2}(1 - y).$$

Using the results of proposition 4.5 we know that higher degree solutions are written

$$Q'(-z) = z^{-2m} Q_{1/2}(-z) + E(z)(1 - z^{-1})^{2k}.$$

Since this is symmetric it can be written as a function of  $\cos(w)$ :

$$Q'_{1/2}(1 - \cos^2(w/2))$$

$$= Q_{1/2}(1 - \cos^2(w/2)) + E_{1/2}(\cos(w)) [\sin^2(w/2)]^k.$$

Clearly, this gives

$$Q'_{1/2}(y) = Q_{1/2}(y) + y^k E_{1/2}(y)$$

where our constraint  $E(z) = E(-z)$  translates to  $E_{1/2}(y) = E_{1/2}(1 - y)$ , giving that  $E_{1/2}(y)$  is symmetric about the point  $1/2$ . The fact that  $E(z)$  is of degree  $4m - 2$  gives that  $E_{1/2}(y)$  has degree  $2m - 1$ . If we alter our notation to use zero phase polynomials throughout we would find  $E(z) = -E(-z)$  or  $E_{1/2}(y) = -E_{1/2}(1 - y)$ , which is precisely the requirement given in [12].

Further, Daubechies gives a closed form for  $Q_{1/2}(y)$ . In our notation this translates to the complementary filter to the binomial.

### ACKNOWLEDGMENT

The authors gratefully acknowledge fruitful discussions with Dr. I. Daubechies, AT&T Bell Laboratories and O. Rioul, CNET, Paris, who also provided the regularity estimates in Section V. They would like to thank J. Kova-

čević and N. T. Thao at Columbia University and the anonymous reviewers for suggesting significant improvements in the manuscript.

### REFERENCES

- [1] J. M. Combes *et al.*, Eds., *Wavelets, Time-Frequency Methods, and Phase Space (Lecture Notes on IPTI)*. New York: Springer-Verlag, 1989.
- [2] P. Goupillaud, A. Grossmann, and J. Morlet, "Cycle-octave and related transforms in seismic signal analysis," *Geoexploration*, vol. 23, pp. 85-102, 1984.
- [3] Y. Meyer, "Orthonormal wavelets," in *Wavelets, Time-Frequency Methods and Phase Space (Lecture Notes on IPTI)*, J. M. Combes *et al.*, Eds. New York: Springer-Verlag, 1989.
- [4] A. Grossmann and J. Morlet, "Decomposition of Hardy functions into square integrable wavelets of constant shape," *SIAM J. Math. Anal.*, vol. 15, no. 4, pp. 723-736, 1984.
- [5] Y. Meyer, *Ondelettes*, vol. 1 of *Ondelettes et Opérateurs*. Paris: Hermann, 1990.
- [6] S. Mallat, "Multifrequency channel decompositions of images and wavelet models," *IEEE Trans. Acoust., Speech, Signal Processing*, vol. 37, pp. 2091-2110, Dec. 1989.
- [7] G. Strang, "Wavelets and dilation equations: A brief introduction," *SIAM Rev.*, vol. 31, pp. 614-627, Dec. 1989.
- [8] E. A. Rosenfeld, *Multiresolution Techniques in Computer Vision*. New York: Springer-Verlag, 1984.
- [9] P. J. Burt and E. H. Adelson, "The Laplacian pyramid as a compact image code," *IEEE Trans. Commun.*, vol. COM-31, pp. 532-540, Apr. 1983.
- [10] S. Mallat, "Multiresolution approximation and wavelets," *Tech. Rep.*, Dep. Comput. Inform. Sci., Univ. Pennsylvania, Philadelphia, PA, Sept. 1987.
- [11] S. Mallat, "A theory for multiresolution signal decomposition: The wavelet representation," *IEEE Trans. Patt. Anal. Machine Intell.*, vol. 11, no. 7, pp. 674-693, 1989.
- [12] I. Daubechies, "Orthonormal bases of compactly supported wavelets," *Commun. Pure Appl. Math.*, vol. XLI, pp. 909-996, 1988.
- [13] O. Hermann, "On the approximation problem in nonrecursive digital filter design," *IEEE Trans. Circuit Theory*, vol. 18, pp. 411-413, May 1971.
- [14] M. J. Shensa, "The discrete wavelet transform: Wedding the á trous and Mallat algorithms," *IEEE Trans. Signal Processing*, to be published, Oct. 1992.
- [15] A. Croisier, D. Esteban, and C. Galand, "Perfect channel splitting by use of interpolation, decimation, tree decomposition techniques," in *Proc. Int. Conf. Inform. Sci./Syst.* (Patras, Greece), Aug. 1976, pp. 443-446.
- [16] R. E. Crochiere and L. R. Rabiner, *Multirate Digital Signal Processing*. Englewood Cliffs, NJ: Prentice-Hall, 1983.
- [17] M. J. T. Smith and T. P. Barnwell, III, "Exact reconstruction for tree-structured subband coders," *IEEE Trans. Acoust., Speech, Signal Processing*, vol. 34, pp. 434-441, June 1986.
- [18] F. Mintzer, "Filters for distortion-free two-band multirate filter banks," *IEEE Trans. Acoust., Speech, Signal Processing*, vol. 33, pp. 626-630, June 1985.
- [19] P. P. Vaidyanathan, "Quadrature mirror filter banks,  $M$ -band extensions and perfect-reconstruction technique," *IEEE ASSP Mag.*, vol. 4, pp. 4-20, July 1987.
- [20] P. P. Vaidyanathan and P.-Q. Hoang, "Lattice structures for optimal design and robust implementation of two-band perfect reconstruction QMF banks," *IEEE Trans. Acoust., Speech, Signal Processing*, vol. 36, pp. 81-94, Jan. 1988.
- [21] M. Vetterli, "Filter banks allowing perfect reconstruction," *Signal Processing*, vol. 10, no. 3, pp. 219-244, 1986.
- [22] M. Vetterli and D. Le Gall, "Perfect reconstruction FIR filter banks: Some properties and factorizations," *IEEE Trans. Acoust., Speech, Signal Processing*, vol. 37, pp. 1057-1071, July 1989.
- [23] T. Q. Nguyen and P. P. Vaidyanathan, "Two-channel perfect-reconstruction FIR QMF structures which yield linear-phase analysis and synthesis filters," *IEEE Trans. Acoust., Speech, Signal Processing*, vol. 37, pp. 676-690, May 1989.
- [24] M. Vetterli and C. Herley, "Wavelets and filter banks: Relationships and new results," in *Proc. IEEE Int. Conf. ASSP* (Albuquerque, NM), Apr. 1990, pp. 1723-1726.

- [25] C. Herley and M. Vetterli, "Linear phase wavelets: Theory and design," in *Proc. IEEE Int. Conf. ASSP* (Toronto, Canada), May 1991, pp. 2017-2020.
- [26] M. Antonini, M. Barlaud, P. Mathieu, and I. Daubechies, "Image coding using vector quantization in the wavelet transform domain," in *Proc. IEEE Int. Conf. ASSP* (Albuquerque, NM), Apr. 1990, pp. 2297-2300.
- [27] A. Grossman, R. Kronland-Martinet, and J. Morlet, "Reading and understanding continuous wavelet transforms," in *Wavelets, Time-Frequency Methods and Phase Space* (Lecture Notes on IPTI), J. M. Combes *et al.*, Eds. New York: Springer-Verlag, 1989.
- [28] A. Cohen, I. Daubechies, and J.-C. Feauveau, "Biorthogonal bases of compactly supported wavelets," submitted for publication.
- [29] O. Rioul, "A discrete-time multiresolution theory unifying octave-band filter banks, pyramid, and wavelet transforms," *IEEE Trans. Signal Processing*, to be published.
- [30] D. Gabor, "Theory of communication," *J. Inst. Elec. Eng.*, vol. 93, pp. 429-457, 1946.
- [31] M. R. Portnoff, "Time-frequency representation of digital signals and systems based on short-time Fourier analysis," *IEEE Trans. Acoust., Speech, Signal Processing*, vol. 28, pp. 55-69, Feb. 1980.
- [32] R. Bracewell, *The Fourier Transform and its Applications*, second ed. New York: McGraw-Hill, 1986.
- [33] I. Daubechies, "The wavelet transform, time-frequency localization and signal analysis," *IEEE Trans. Inform. Theory*, vol. 36, pp. 961-1005, Sept. 1990.
- [34] N. Dyn and D. Levin, "Interpolating subdivision schemes for the generation of curves and surfaces," *School Math. Sci.*, Tel Aviv Univ., 1990, preprint.
- [35] O. Rioul, "Dyadic up-scaling schemes: simple criteria for regularity," *SIAM J. Math. Anal.*, to be published, 1992.
- [36] A. Cohen, "Ondelettes, analyses multirésolutions et traitement numérique du signal." Ph.D. dissertation, Université Paris IX Dauphine, 1990.
- [37] M. J. T. Smith and T. P. Barnwell III, "A procedure for designing exact reconstruction filter banks for tree structured subband coders," in *Proc. IEEE Int. Conf. ASSP* (San Diego, CA), Mar. 1984, pp. 27.1.1-27.1.4.
- [38] P. P. Vaidyanathan, "Multirate digital filters, filter banks, polyphase networks, and applications: A tutorial," *Proc. IEEE*, vol. 78, pp. 56-93, Jan. 1990.
- [39] V. Belevitch, *Classical Network Synthesis*. San Francisco, CA: Holden Day, 1968.
- [40] P. P. Vaidyanathan and Z. Doğanata, "The role of lossless systems in modern digital signal processing," *IEEE Trans. Education*, vol. 32, pp. 181-197, Aug. 1989.
- [41] A. V. Oppenheim and R. W. Schaffer, *Digital Signal Processing*. Englewood Cliffs, NJ: Prentice-Hall, 1975.
- [42] I. Daubechies, "Orthonormal bases of compactly supported wavelets II: Variations on a theme," 1989, AT&T preprint.
- [43] M. R. Schroeder, *Number Theory in Science and Communications*, second ed. New York: Springer-Verlag, 1986.
- [44] T. Kailath, *Linear Systems*. Englewood Cliffs, NJ: Prentice-Hall, 1980.
- [45] A. J. E. M. Janssen, "Note on a linear system occurring in perfect reconstruction," *Signal Processing*, vol. 18, no. 1, pp. 109-114, 1989.
- [46] R. Blahut, *Fast Algorithms for Digital Signal Processing*. Reading, MA: Addison-Wesley, 1984.
- [47] J.-C. Feauveau, "Analyse multirésolution par ondelettes non orthogonales et bancs de filtres numériques," Ph.D. dissertation, Université de Paris-Sud, 1990.
- [48] D. E. Knuth, *The Art of Computer Programming: Seminumerical Algorithms*, vol. II, second ed. Reading, MA: Addison-Wesley, 1981.
- [49] A. Y. Khinchin, *Continued Fractions*. Chicago, IL: University of Chicago Press, 1964.
- [50] E. W. Cheney, *Introduction to Approximation Theory*, second ed. New York: Chelsea, 1981.
- [51] C. Herley and M. Vetterli, "Biorthogonal bases of symmetric compactly supported wavelets," in *Wavelets, Fractals and Fourier Transforms*, M. Farge, J. C. R. Hunt, and J. C. Vassilicos, Eds. Oxford University Press, to be published 1992.
- [52] R. A. Gopinath, personal communication, July 1990.



**Martin Vetterli** (S'86-M'86-SM'90) was born in Switzerland in 1957. He received the Dipl. El.-Ing. degree from the Eidgenössische Technische Hochschule Zürich, Switzerland, in 1981, the master of science degree from Stanford University, Stanford, CA, in 1982, and the Doctorat ès Science degree from the Ecole Polytechnique Fédérale de Lausanne, Switzerland, in 1986.

In 1982, he was a Research Assistant at Stanford University, and from 1983 to 1986 he was a Researcher at the Ecole Polytechnique. He has worked for Siemens and AT&T Bell Laboratories. In 1986, he joined Columbia University in New York where he is currently Associate Professor of Electrical Engineering, a member of the Center for Telecommunications Research, and Codirector of the Image and Advanced Television Laboratory. His research interests include multirate signal processing, wavelets, computational complexity, signal processing for telecommunications, and digital video processing.

Dr. Vetterli is a member of SIAM and ACM, a member of the MDSP Committee of the IEEE Signal Processing Society and of the editorial boards of *Signal Processing*, *Image Communication*, and *Annals of Telecommunications*. He received the Best Paper Award of EURASIP in 1984 for his paper on multidimensional subband coding, and the Research Prize of the Brown Boverly Corporation, Switzerland, in 1986 for his thesis, and the IEEE Signal Processing Society's 1991 Senior Award (DSP Technical Area) for a 1989 transactions paper with D. LeGall on FIR filter banks.



**Cormac Herley** was born in Cork, Ireland, in 1964. He received the B.E. (Elec.) degree from University College Cork in 1985, and the M.S.E.E. degree from the Georgia Institute of Technology, Atlanta, in 1987. Since 1990 he has been working towards the Ph.D. degree in the Department of Electrical Engineering, Columbia University, New York, NY.

From 1987 to 1989 he was employed at Kay Elemetrics Corp., New Jersey. He is now a Research Assistant at the Center for Telecommunications Research, Columbia University.